UNIVERSITA' DEGLI STUDI DI PARMA

DOTTORATO DI RICERCA IN
"MEDICINA MOLECOLARE"

CICLO XXX

THREE-DIMENSIONAL METHODOLOGY FOR STEREOPHOTOGRAMMETRIC ACQUISITION OF THE SOFT TISSUES OF THE FACE

Coordinatore:
Chiar.mo Prof. Luciano Polonelli

Tutore:
Chiar.mo Prof. Guido Maria Macaluso

Dottoranda: Dott.ssa Marisabel Magnifico

Anni 2014/2017

È stato decisivo, per l'impostazione tematica e la realizzazione della tesi, l'impegno in questa profuso dal Prof. Guido Maria Macaluso, dal Prof. Mauro Gandolfini e dal Prof. Alberto Di Blasio, ai quali mi lega un felice rapporto di sostanziale condivisione dell'attività di ricerca svolta, che ha potuto così giovarsi del prezioso contributo della loro elevata professionalità, del quale io personalmente li sono profondamente grata.

SUMMARY

1. INTRODUCTION

The quantitative analysis of the human face has always received a large attention from both scientists and artists: the face allows to communicate and interact with the environment and it is used to identify the persons, and it can carry information about the health state of an individual[1].

The face represents the bodily district that, most of all, identifies and characterizes the person[2]; it is a site of vital functions for the body (e.g. breathing and feeding) and plays a key role in recognition, expression, mimicry and social communication[3]. Quantitative analysis of the face is a daily process, often unconscious[4]. The same process is carried out by several medical specialists, using techniques that require accuracy and precision[5]. In this way aesthetic and maxillofacial surgeons, otolaryngologist, dentists, oral surgeons, orthodontists can both document clinical cases and compare different images of the same patient (e.g. pre- and post-treatment).

Until the 19th century, these assessments were carried out directly on the patient, using the calibre or instruments that could be referred to. In recent times, photographs and analogue x-rays have been used to separate the moment of image acquisition from that of its analysis. The advent of digital technology, both in photographic and radiographic environments, has allowed to acquire, manage, process, analyse and archive a large amount of images and data.

Today, we have more sophisticated techniques that added to our evaluations the third dimension (3D) and even more recently the fourth dimension (4D) that is the movement.

Speaking a "three-dimensional" language means approaching reality; classic photographs and radiographs, in fact, are nothing more than two-dimensional artifices, capable of representing on a sheet, film or screen, a reality that is three-dimensional.

Anthropometry, which was developed in the late 19th century, is the biologic science of measuring the human body and its characteristics[6]. Although its applications are usually medical, today it also plays an important role in commercial settings, such as clothing design, ergonomics, and architecture. In cranio-maxillofacial and plastic surgery anthropometry is especially challenging because of the

complex structures of the face, which do not allow an assessment with simple measurements. An objective, accurate, and reliable system for quantifying the soft tissues of the face in dimension and colour is still needed[7]. Interest in overcoming the limitations of direct measurements and of two-dimensional photography has led to the development of numerous three-dimensional scanning devices.

Kau *et al*[8] give an overview of the three-dimensional scanning device types available. Despite the huge amount of literature about the new three-dimensional system, a clear and objective evaluation of accuracy and reliability under different circumstances is missing for many of them. The aim of this work was to evaluate the precision and the accuracy of a new stereophotogrammetric system.

1.1 Anthropometry in orthodontics and maxillo-facial surgery

Anthropometry is the measurement of the human body as a whole (stature, weight) and of its segments (head, trunk, limbs), whose dimensions are measured in terms of distances between anatomical references or architectural points (cephalometric and somatometric points), and calculate the reciprocal dimensional ratios expressed as a percentage (anthropometric indexes)[9]. It is a technique that allows to quantify the shape of the body.

The existence of biological differences among various populations has become apparent when men began migrations. Linneo's classification[10] included several human groups in its taxonomy of species, defined quantitatively only in the nineteenth century in Quetelet's studies[11] on chest measurements of 5.738 Scottish soldier, that concluded that these measures had a distribution around an average that followed the error law.

Anthropometric measurements such as the size of the head, trunk and limbs have been the basis of racial diversity studies already in the 18th century[12]. Their use has been extended to determination of healthy or strong physicist and hence their application in assessing the physical quality of slaves and recruits to the armies of Europe and North America. Finally, it was used to investigate the state of

well - being of both adults and children in general populations[13,14]. Their use in this field has increased in the second half of the 20th century, becoming an integral part of epidemiological studies[15,16].

This led to the definition of anthropometry in the 20th century as "a system of techniques, the systematic art of measuring man, his skeleton, his brain and other organs, through the most appropriate means and methods"[17].

In particular, body measurements are used for example in legal anthropometry to identify age[18], sex, and race[19,20]; in orthopaedics are useful for drawing proper prostheses[21]. Sports anthropometry has been relevant in the selection of athletes and team sports in determining roles[22].

Anthropometry is of great importance in pregnancy, where assessments of the mother[23,24] and the fetus[25,26] allows to make predictions about the health status of the child[27], whether in the pediatric field where it is essential to monitor child's state of health or to control the progression of various pathologies[28].

In maxillo-facial surgery and orthodontics, anthropometry plays a key role in the analysis of hard and soft tissues; cephalometric study and 3D images are an excellent aid for diagnosis and therapeutic planning, to investigate the face and asymmetry of the face, and especially to monitor facial changes during a treatment[29,30,31,32].

Unfortunately, cephalometric analysis has several limitations in treatment planning, especially for aesthetic reasons[33,34]. For example, the soft tissue covering the teeth and the bone may have so significant variations changes to make inadequate the appreciation of facial disharmony through only the dento-skeletal model[35].

Many key principles of this discipline derive from evaluations performed on "harmonic" patients. When these "normal values" are applied in presence of vertical or antero-posterior skeletal disharmony they seem to lose their reliability.

Burstone[36] said that only correcting dental discrepancy does not allow to modify facial aesthetics and in some cases even cause new disagreements. Another source of error is the use of the skull base as

a reference line for measuring the facial profile. Michiels[37] found that the measures involving the skull base are less accurate than those involving intermaxillary relationships.

For these reasons, many authors[38,39,40] have suggested the use of soft tissue analysis as a reliable guide for treatment planning both at occlusal level and obviously in face aesthetics.

In particular, G.W. Arnett[41] has studied how cephalometric analysis of soft tissues can be used to examine five different but interconnected domains:

- Dento-skeletal factors. These have a great influence on the facial profile; under normal conditions, usually produce a balanced and harmonious relationship between nasal base, lip, skin point A and B and chin. The accuracy of the orthodontist and surgeon in the management of these components will greatly affect the end result;
- Characteristics of soft tissues. The thickness of the upper lip and lower lip (analyzed by calculating the distance between points B and cutaneous point B, Pogonion and cutaneous Pogonion, Menton and coutaneous Menton) alters the facial profile (Fig. 1). In the lower third of the face, the soft tissue thickness is, together with the respective dento-skeletal points, among the greatest responsible for aesthetic equilibrium. The nasolabial angle is influenced by the position of the upper incisors and the thickness of the soft tissue overlying them;

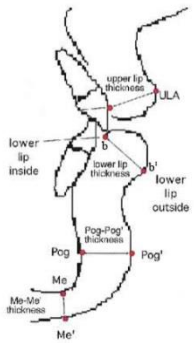

Figure 1. Soft tissue structures and thicknesses, and dentoscheletric factors that determine the profile.

- Length of the face. It is mainly studied by analysing the vertical size of the upper and lower lip soft tissues, the interlabial gap, the lower third of the face, and the total facial height. The

presence and position of any vertical anomalies are evaluated through overbite, maxillary and mandibular height and upper incisor exposure;

- Projection on the vertical line of the face. This is identified as the line perpendicular to the passing horizon for the subnasal point. The horizontal distance for each point of reference, measured perpendicular to that line, defines its absolute value. For an accurate clinical examination of the patient, these evaluations must also be carried out as described by Arnett and Bergman;
- Harmony between the parties. A key role in perceiving the beauty of a face is played by harmony and balance between different facial points of reference. Harmony values represent the horizontal distance between 2 points measured perpendicular to the vertical line of the face. Four equilibrium areas have been identified: 1) intramandibular, 2) intermaxillary, 3) orbital-maxillary, 4) face in its entirety;
- Arnett e da Bergman[42,43] have highlighted how to diagnose and treat malocclusions orthodontists should use dental and facial keys. Dental keys (overjet, canine occlusion and molar occlusion) often play a dominant role in determining the treatment, while the face keys (relative positions of the upper lip, lower lip and chin) are often used sparingly or even not used at all. They have thus presented an organized and complete analysis in order to detect the correct facial traits and modify that by orthodontics and surgical procedures. The simple correction of a Class I occlusion patient can lead to different aesthetic results, and often unsatisfactory. Among the various analyses suggested, the most important is the assessment of facial form and asymmetry through the evaluation of lines such as *Trichion-Menton* cutaneous, *Zygion-Zygion* or bipupillary. It is also useful to divide the face into three thirds: the upper between the line passing through *Trichion* and the eyebrow, the middle third from the eyebrow line to the passing line for the *Subnasale* point and the lower one from *Subnasale* to the straight line passing for coutaneous *Menton*. To check the presence of asymmetries

between the thirds of the face, it is also used the interpupillar line together with the upper and lower intercanine lines and *menton* line (Fig. 2).

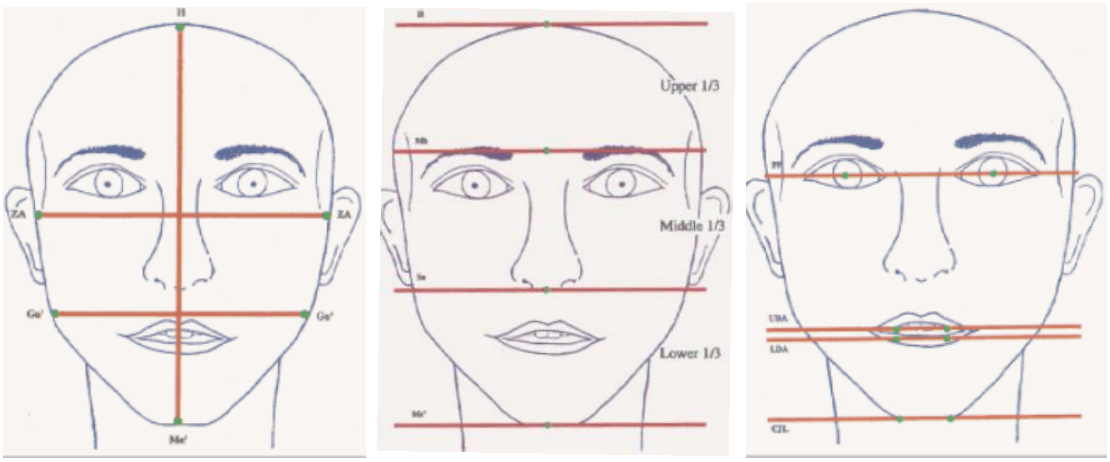

Figure 2. Clinical evaluation of facial form and asymmetry.

On the profile patient's face we can evaluate the profile angle (formed by the points *Glabella-Subasion- Pogonion*), the nose-lip angle (formed by lower nasal septum-*Subnasion*-anterior point of the upper lip), the contour of the jaw and mandibular lobe (whose punctual measurement is not possible but a simple clinical evaluation) and the Cheekbone contour (Fig. 3).

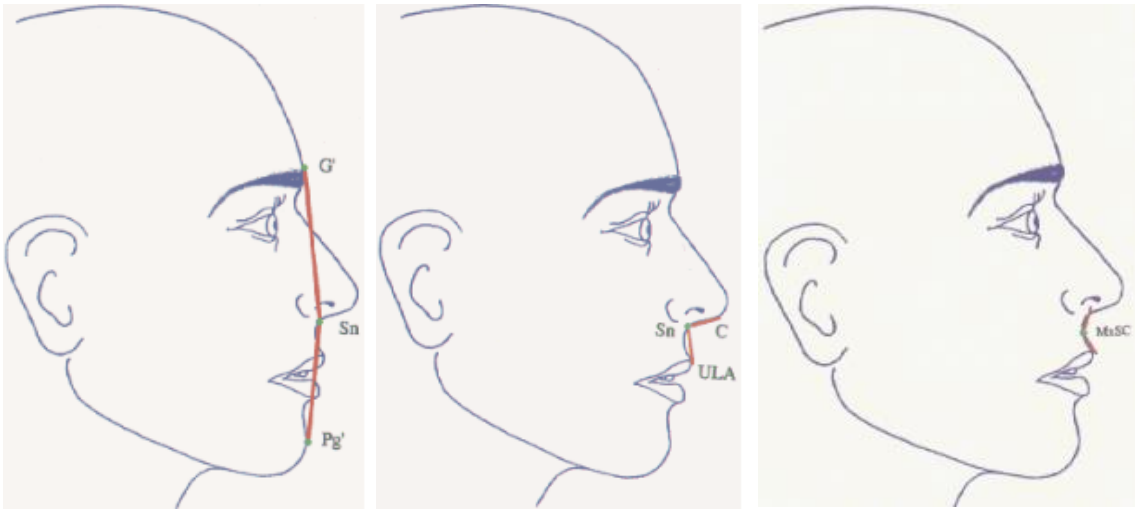

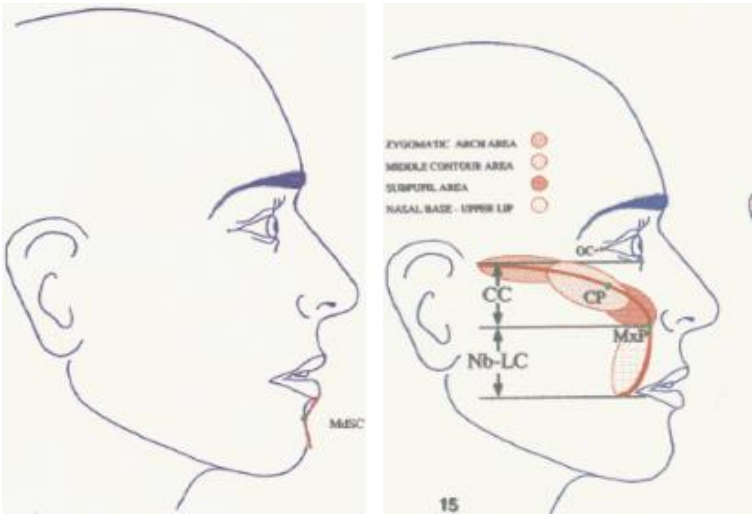

Figure 3. Analysis of facial profile.

1.2 Three-dimensional imaging of the face

The primary objective of the traditional orthodontic diagnosis and treatment planning termed the "Angle paradigm" was ideal dental occlusion and acceptable skeletal relationship. Today, the importance of soft tissue is better understood and improvement in facial appearance is one of the most important factor for patients seeking orthodontic treatment. With the paradigm shift from hard tissue to soft tissue, the key determinant in orthodontic diagnosis and treatment success now lies behind soft tissue positions[44]. With an objective evaluation of soft tissue an efficient treatment planning can be made, and the patients can be accurately assessed at the end of the treatment. The paradigm shift necessitates using three-dimensional (3D) imaging, because traditional two-dimensional (2D) cephalometry places emphasis on hard tissue landmarks, because their reproducibility is better than soft tissue landmark[45].

Various methods have been used to measure facial soft tissues: direct anthropometry, two-dimensional photogrammetry, lateral cephalometry, cone beam computed tomography (CBCT), and surface scanning methods (laser scanning, moiré topoghraphy and 3D stereophotogrammetry). The rapid development of 3D imaging system has enabled us to diagnose facial soft tissue in detail and open a new window for 3D soft tissue evaluation in orthodontic planning and treatment results.

Direct anthropometric measurement is a reliable and affordable method. Farkas *et al*[46] conducted important studies to create a large database of direct anthropometric measurements that can be used for facial measurements. Direct anthropometry, which is considered as gold standard for facial measurements, has some disadvantages; for example, it is time consuming and requires patient compliance. Frontal and profile photographs are generally used for photogrammetric measurement. Two-dimensional images (photograph, lateral cephalometry) are a snapshot of a dynamic object and, therefore, required cooperation only during acquisition and are easier to obtain than direct measurement[47]. On the other hand, with 2D imaging methods, magnification and distortion problems may occur and many variables can affect measuring standardization, such as illumination variations and object-camera distances. Furthermore, evaluation of the 2D cross-sectional images of a 3D object has significant inadequacies[48].

From the introduction of cephalostat, Broadbent stressed the importance of coordinating the lateral and postero-anterior cephalometric films to arrive at a distortion-free definition of skeletal craniofacial form[49]. The first reports on implementation of this method were by Singh and Savara[50] on 3D analysis of maxillary growth changes in girls. The earliest clinical use of stereophotogrammetry was reported by Thalmann-Degan in 1944 (according to Burke and Beard[51]) who recorded change in facial morphology produced by orthodontic treatment.

On the other hand, the first commercial Computerized Tomography (CT) scanner appeared in 1972. Soon after, it was apparent that a stock of CT sectional images could be used to generate 3D information. In the 1980s, researchers began investigating 3D imaging of craniofacial deformities. The first simulation software was developed for craniofacial surgery in 1986. Shortly after, the first textbooks on 3D imaging in medicine appeared with a concentration on the principles and applications of 3D CT- and MRI-based imaging. Three-dimensional imaging has evolved into a discipline of its own, dealing with various forms of visualizations, manipulations and analysis of multi-dimensional medical structures[52].

Face growth, development and aging produces a never static outline that can be modelled and varied by the combined action of different factors. Additionally, the presence of a large number of facial muscles makes facial appearance instantaneously variable and dynamic, even producing problems for its correct representation and measurement.

Three-dimensional (3D) images has evolved greatly in the last two decades and has found applications in orthodontics, oral and maxillofacial surgery. The application include pre- and post-orthodontic assessment of dentoskeletal relationship and facial aesthetic, auditing orthodontic outcomes with regard to soft and hard tissue, 3D treatment planning, and 3D soft and hard tissue prediction (simulation). Three-dimensionally fabricated custom-made archwires, archiving 3D facial, skeletal and dental records for in-treatment planning, research and medico-legal purpose are also among the benefits of using 3D models in orthodontics[53].

1.3 General 3D concept

Before exploring the different techniques available, it is necessary to understand some of the principles and terminology in 3D imaging. 3D models are generated in several steps. The first step, 'Modeling', uses mathematics to describe the physical properties of an object. The modeled object can be seen as a 'wireframe' or a 'polygonal mesh'. The mesh is usually made up of triangles or polygons and it is used as mode of visualization. A part of the modeling procedure is to add a surface to the object by placing a layer of pixels and this is called 'image' or 'texture mapping'. The second step is to add some shading and lighting, which brings more realism to the 3D object. The final step is called 'rendering', in which the computer converts the anatomical data collected from the patient into a life-like 3D object viewed on the computer screen.

3D imaging approaches are generally classified into three categories:

- slice imaging, e.g. a set of CT axial data to produce reconstructed 2D images;
- projective imaging, e.g. surface laser scanning to produce what is considered a 2.5-D mode of visualization;

- volume imaging, e.g. holography or ‘varifocal mirrors’ techniques.

For measuring scanned objects in 3D, there are two main geometrical strategies: orthogonal measurements and measurement by triangulation[54]. Orthogonal measurements means that the object is slice into layers. The x and y dimensions are measured directly on the slice surface, and the z dimensions is measured by tallying the number of slices in the area of interest (e.g. CT scan). Measurement by triangulation is analogous to the geometry of mammalian stereoscopic vision. Simply, two images of the object need to be captured from two different views simultaneously or in a rapid succession.

Currently, two image analyzers can provide combined 3D reconstructions of the soft tissue structures together with the craniofacial skelston: computer tomography (CT) and magnetic resonance (MR). These volumetric scanners can image both the internal body structures and the external coutaneous covering, allowing a complete assessment of facial morphology. Other scanners (laser scanner and stereophotogrammetric system) can record and reproduce only the external body surface, permitting 3D measurements of the soft tissue[55].

CT provides 3D digital reconstruction of the entire craniofacial skeleton from axial slices allowing to evaluate all internal structures. This technique has gained considerable popularity and applications in the medical field for trauma, fractures or neoplasias, but with regard to facial imaging, its main disadvantage are:

- patients exposure to a high dose of ionizing radiation;
- limited resolution of facial soft tissue due to slice spacing;
- the possibility to have artefacts created by metal objects inside the mouth.

The most recent modification of CT, namely conical x-ray approach or cone bean CT (CBCT), now can offer affordable 3D craniofacial reconstructions, with a reduced radiation exposure. CBCT system have been developed specifically for the maxillofacial region, and their field of view allows an efficient imaging od the skull including most of the landmarks used in cephalometric analysis, together with a 3D volumetric rendering of the external facial surface[56].

RMN is a technique based on the measurement of the precession spin of nuclei equipped with magnetic moment when they are subjected to a magnetic field[57]. It does not use ionizing radiation, but only a strong magnetic field, so it is considered non-invasive but cannot be used in patients with pacemakers, vascular clips, and pregnant women. With this method, the soft tissues can be thoroughly analysed but excessive costs make difficult to use it for routine use in anthropometric research. Magnetic resonance imaging should be performed in a supine position, with a significant alteration in the normal relationship between the facial soft tissues, especially in the aged persons[58].

1.4 Soft tissue imaging techniques

There are several methods for capturing object-related data, some direct (where physical contact between subject and mapping system is required) and some indirect (where contact is not necessary) (Table 1). The latter are more accurate because they do not deform the surface during measurements and are also effective for the most difficult measurements, such as those related to the eyes, without causing discomfort or possible damage to the patient[59,60,61]. There are several studies in the literature that have analysed the different modes of acquisition of soft tissue of the face such as photography[62,63,64], nuclear magnetic resonance imaging (RMN)[65], 3D photography[66,67], 3D ultrasonography[68] and 3D laser scanners[69,70]. 3D imaging techniques exploit several physical principles to rebuild the three-dimensional image.

Soft tissue acquisition	*Advantages*	*Disadvantages*
2D Photography	Accurate Easy Low cost	No 3D Volumetric CT (CB) data needed to match surface texture
RMN	Low cost No ionizing radiation	Long acquisition time No surface texture Soft tissue deformation due to position High cost
3D Ultrasonography	Low cost No ionizing radiation	Long acquisition time No surface texture Deformation of soft tissue due to contact between probe and skin

3D Laser scanner	Accuracy of the data	Harmful to eyes Long acquisition time Multiple scanners needed to acquire surface textures High cost Negative light and metal objects
3D Phtography Stereophotogrammetry	No radiations Accurate and metric data are correct Short capture time (2 ms) Surface textures of soft tissues Low cost	Poor precision in eye reproduction Poor accuracy of the subnasal and submental areas

Table 1. Features of the different soft tissue imaging techniques [71].

3D Ultrasonography

3D ultrasonography is based on computer reconstruction and processing of normal two-dimensional ultrasound images. The main limitations of this technique are due to tissue deformation at the passage of the probe and the lack of a precise surface texture; this means that, despite the low costs, this technique is not considered sufficiently accurate for the acquisition of soft tissue data.

3D Laser scanners

Laser scanners are another well-known class of instruments that can be used for surface analysis. The instruments shines a low-intensity laser (below 0.00008 W) on the object and digital cameras capture the images; the depth information is obtained by triangulation geometry[72]. During data acquisition, either the face or the laser light move to cover the entire surface (approximately in 17s, with a scanning precision of 0.65 mm, mean scanning error of 1.0-1.2 mm and a recording error of 0.3-0.4 mm). It provides a less invasive method of capturing the face for planning or evaluating outcome of orthodontic or orthognathic surgical treatment. However, this technique has several shortcomings for facial scanning. They include the slowness of the method, making distortion of the scanned image likely, safety issue related to exposing the eyes to the laser beam, inability to capture the soft tissue surface texture, which results in difficulties in identification of landmarks that are depended on surface colour.

3D laser scanner acquires a point cloud limited to the instrument scan window and this often leaves a part of the object in the shade. This technique is great for rigid objects, with few underlays and motionless, because any motion during the relatively long scan time would damage the quality of the result. Even though no radiation is emitted, you should use this tool carefully because it is potentially damaging to your eyesight if your eyes are kept open when capturing images.

Structured light techniques

In the structure light technique, the scene is illuminated by a light pattern and only one image is required (compared with the two image with stereophotogrammetry). The position of illuminated points captured image compared to their position on the light projection plane provides the information needed to extract the 3D coordinates on the image object[73]. However, to obtain high-density models, the face needs to be illuminated several times with random patterns of light. This increases the capture time with increased possibility of head movements. In additions, the use of one camera does not provide a 180° (ear to ear) facial model, which necessitates use of several cameras or rotating the subjects around an axis of rotation, which is not practical and has resulted in reduced applicability of this technique[74].

2. STEREOPHOTOGRAMMETRY

Sterophotogrammetry is safe, non-invasive, fast (typical scan time 2 ms), does not require a physical contact between the instrument and the face, and it provides superior quality "external surface" photographs, coupling a color facial image (texture) with a 3D mesh of the analysed surface. In stereophotogrammetry a light source illuminates the face, and two or more coordinated cameras (or set of cameras) record the images from different points of view. The different views/images of the face are merged into a 3D point cloud to represent the surface of the subject's face. Using a previous calibration of the instrument, a computerized stereoscopic reconstruction of the face is finally produced[75,76]. Two additional three-quarter color pictures are mapped onto the mesh formed by the point cloud to reproduce facial appearance. The system can be divided into passive, where the camera record the black and white (finer resolution) and the color (lower resolution) images of the face that are combined to give a final 3D mesh covered by a color texure, or active. In these last instruments, the face is also lightened by structured light (usually in the infrared field), whose interferences with the facial structures enhance the final 3D reconstruction. Precision (difference between repeated measures of the same item) and repeatability (precision relative to the actual biological difference among subjects) of stereophotogrammetry have been reported to be very satisfactory, even better than caliper measurements[77,78,79]. Ras *et al*[80] have demonstrated a stereophotogrammetric system that gives the three dimensional coordinates of any chosen facial landmark, so linear and angular measurements could be calculated to detect any changes in facial morphology. Previous making of the landmarks of interest increases the instruments precision, without reducing the information content of the acquired 3D image[81]. Indeed, some landmark can be efficaciously identified only with palpation of the underlying bone surface, a procedure that cannot be performed on the facial scan. For instance, the error of *gonion* identification was 2-4 times larger than that of the other facial landmarks. Other landmarks (*tragus, menton, orbitale superior*) were of difficult identification because the facial region is covered by hair, or because the scan was not optimal[82].

Due to its safety, the fine resolution images and the acquisition time, the instrument is ideal to collect the 3D data of faces, even in children, babies or disabled persons, where acquisition tims is going to be critical. The instrument can be used also for the digital analysis and reconstruction of other body regions, like the head and the neck[83,84].

In this technique, 3D information is obtained by capturing and comparing a certain number of photographic images processed on the basis of principle of triangulation (for which, given the sum of the internal angles of a triangle of 180°, it is possible to calculate the distance between the vertices knowing the underlying angles and vice versa). The same principle is the basis for binocular or stereoscopic vision; thanks to the fusion of two different images from each eye, our brain is able to reconstruct the three-dimensional image of the objects it is seeing.

2.1 Historical notes

Binocular vision and three-dimensional perception of the reality surrounding men has been the interest of several scholars and artists throughout the whole history of humanity. Among the many, there are Euclid and Leonardo da Vinci.

With Euclide, the optic is for the first time structured in axioms and theorems: in its work, *Ottica e Catottrica*, there are elements of perspective, the study of reflection in the planar and spherical mirrors and is defined the concept of "visual ray" as without physical structure.

The first postulate of this work, concerning the rectilinear propagation of visual rays emitted by eye, is the foundation of the Euclidean geometric optic, placing both the concept of ray as the way of light propagation mode and the concept of straight propagation. The nature of such axioms, however, is strongly conditioned by the idea that the vision is made by rays emitted from the eye. On the other hand, the definition of ray as a mathematical entity together with the idea that a ray cone may be emitted from the eye, with vertices in the eye and the base on the object, are in fact an innovation methodological approach that makes it possible to extend the *mos geometricus* to the optic.

The understanding of the optic was clinging to the ancient Platonic and Aristotelian beliefs that human beings perceived the universe because the eye projected particles that were then re-reflected to the eye. It was thanks to the studies of Leonardo and Leon Battista Alberti that the concept of an undulating nature of light was introduced and that this came from objects instead of running.

Leonardo was almost certainly the first to write about stereoscopic vision and how the eyes, by virtue of being two, collect information about an object. He also understood that this information was then transmitted to be interpreted "by the soul," or from what we know today as the brain cortex, that is, the brain region responsible for processing the incoming sensory information.

The interest in stereoscopic vision resumed around the middle of 1800 when Sir Charles Wheatstone made the first stereoscopic experiments with pairs of pictures slightly different from one another to reproduce the two images perceived by the human eye . For the visualization of these first "stereographic" drawings, he invented an instrument composed of mirrors and prisms that he proposed to call "stereoscopic" (Fig. 4a).

a 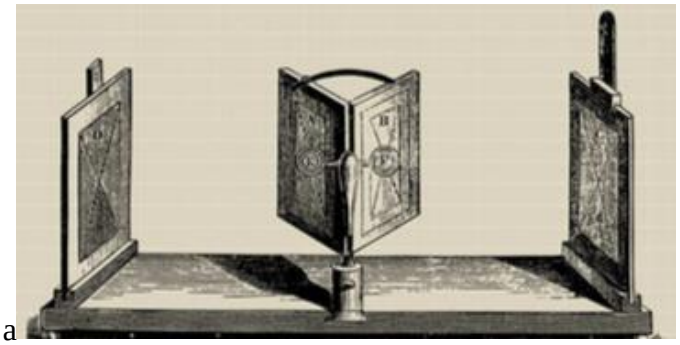 b 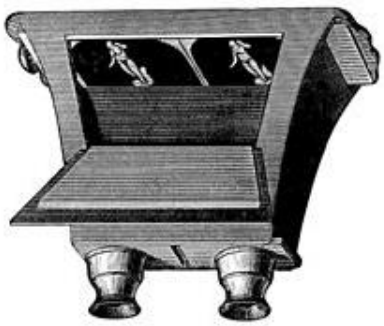

Figure 4. a) Charles Wheatstone mirror stereoscope b) David Brewster stereoscope.

The updated version of the stereoscope, by David Brewster (1849) was a great success: it was a lighter and more practical tool with lenses through which to look at a couple of photographs, made with a binocular camera, placed at the other end of the appliance (Fig. 4b).

In the twentieth century, stereoscopy is developed in different directions: on the one hand the stereoscope uses photographic films and meets commercial evolution, on the other hand cinema is

increasingly interested in this technology and, passing through the first films made with binocular film , you get to current technologies that match (double objective) or alternate (single goal) visions for the right and left eye.

Currently, the main scope of the stereoscopic principles remains the topographic survey of the territory (aerial-photography) for cartographic and archaeological purposes and, in the architectural field, the detection of the space coordinates of existing or virtually reconstructed buildings.

In medicine, stereophotogrammetry applications are becoming increasingly popular since the commodity of these instruments has met the clinical needs of many specialists. In many areas, it is imperative to have images as close to reality as possible: plastic, reconstructive and aesthetic medicine[85], maxillo-facial surgery, orthodontics[86] and other branches of dentistry[87] only to cite face-related disciplines. The images play a key role from diagnosis, nosological framing, communicating with the patient, and then documenting the entire medical-surgical procedure at all stages from intervention to follow-up.

2.2 Modern stereophotogrammetry

As with binocular vision also in artificial "photogrammetric" system, the position of a point is localized by pairs of cameras. For each pair of cameras rigidly fixed in a known position, for each corresponding point p (x, y) in the two images, it is possible to calculate the third coordinate z as the value of b in the triangle, knowing the distance and angles between the cameras h, α, β) (Fig. 5) by the formula:

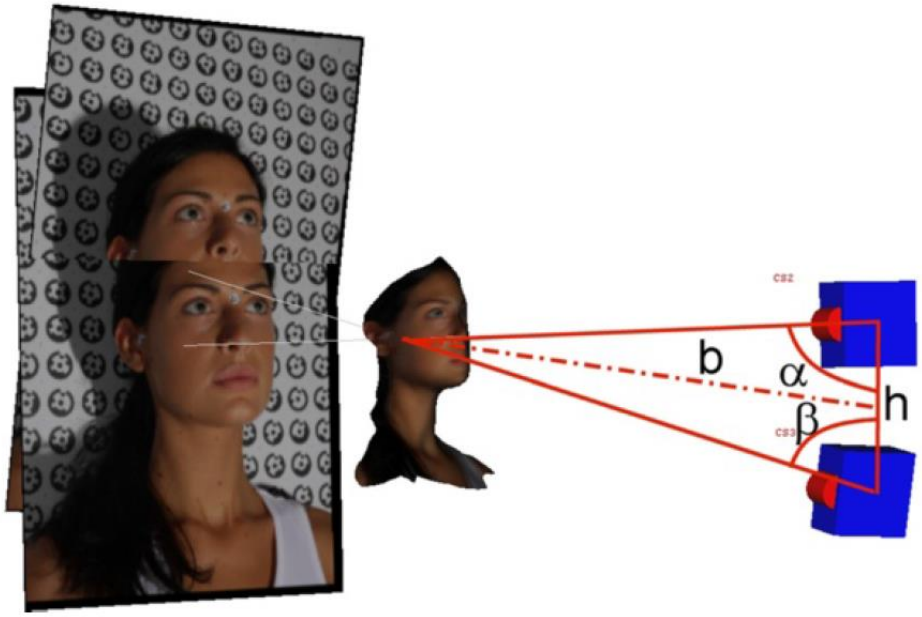

Figure 5. Principle of triangulation used in stereophotogrammetry.

$$b = y \cdot \tan\beta$$

$$b = x \cdot \tan\alpha$$

where *x* and *y* are the segments linking respectively α and β at the point of intersection of b with h. The system is thus obtained:

$$\begin{cases} x + y = h \\ y \cdot \tan\beta = x \cdot \tan\alpha \end{cases}$$

which can be resolved by *x* or *y*, finally finding

$$b = \frac{l \cdot \tan\alpha \cdot \tan\beta}{\tan\alpha + \tan\beta}$$

knowing that $\tan\alpha = \sin\alpha / \cos\alpha$ and $\sin(\alpha + \beta) = \sin\alpha\cos\beta + \cos\alpha\sin\beta$ this expression can be modified as follows:

$$b = \frac{h \cdot \sin\alpha \cdot \sin\beta}{\sin(\alpha + \beta)}$$

this results in the measurement of the height *b* of the base triangle *h*.

The photographs must be taken from at least two different positions so that, by superimposing the images, it is possible to define the 3D coordinates of the points of interest and thus the shape and size of the object. In this way a 3D model of soft facial tissues can be obtained, represented by a cloud of points determined based on their spatial coordinates. By connecting and recognizing the features that link these 3D points to the cloud, a mesh is created, that is a face reconstruction made of small polygons. Finally, a software processes the image.

'Photo-based scanning' uses digital cameras and a processing algorithm that compares pairs of images based on small portions (or patches), area by area, evaluating which patch matches another. Once optimal matching is defined, the position and orientation already calculated for the photographs are used to calculate the location of the patch in 3D space.

The precision and reliability of 3D measurements of facial soft tissues were evaluated by Swennen *et al*[88] by comparing data obtained on the same sample of subjects using CT tomography and 3D stereophathogrammetry.

TC facial soft tissue measurements showed great accuracy except for the areas of hair attachment, eyebrows and eyelids. In contrast, 3D stereofotogrammetry has shown great precision and reliability, except for bone support points (*Gonion, Zygion*). Also a study conducted by Metzer *et al*[89] has confirmed that there are no significant differences between the two methods, except for some areas where stereophotogrammetry seems inferior; however, the differences are clinically acceptable from the orthodontic point of view. For this reason, these two techniques are often associated to achieve a highly accurate three-dimensional reconstruction[60,61,90].

3D photography is the most accurate method for facial anthropometry, being simple, safe, non-invasive, fast, accurate, economical, and free from ionizing radiation. Among all the three-dimensional detection methods, stereophotogrammetry is the only one that allows simultaneous acquisition of a wide, curved surface in a very short time (from 1/100 to 1/5000 seconds)[91].

2.3 Tools, applications and fields of use

- *Assessment of facial deformity, and the outcome of surgical and/or orthodontic correction*. 3D models are very valuable media for locating the source of deformity and its magnitude. Three-dimensional models can be manipulated in any direction, which give considerable informations to the orthodontist without the need for patients recall or being restrict by the time of clinical assessment. Assessment of outcome can also be performed easily by visual comparison of pre- and post- treatment models placed side by side.

For the objective assessment of facial morphology and facial changes following orthodontic and/or surgical interventions, different methods and analyses have been proprosed: landmarks'displacements[92], interlandmark distances and angles, color-millimetric maps[93], and volumetric changes[94,95].

- *Fusion of images from different sources.* While CT scans offer a detailed image of the skeletal surface and volumes, 3D facial images obtained by an optical method can provide additional information about color and surface texture, as well as higher resolution of soft-tissue surfaces. The two methods may therefore be combined, providing a more complete assessment of the patients. The fusion can be made using landmarks or surface-based method that are currently provided by some software tools, but the soft tissue structures may not be stable enough as references, thus including an unknown amount of error[96].

One-step towards a possible solution of the problem is the definition of a good set of fiducial landmarks that is points imaged with both techniques that act as reference for the subsequent superimposition of the digital image[97]. Boulanger *et al*[98] matched CBCT and stereophotogrammtric scans using a set of titanium targets. Surface matching between homologous areas of couples of 3D facial images has been found to be effective, with average deviations between repeated scans lower than 1 mm. A combined use of fiducial landmarks (manual selection and initial matching) and of facial areas that were not modified by the treatment (manual selection and automatic fine matching)

is usually employed for longitudinal investigation[99]. Another field of interest is the fusion protocol that integrated a digital dental cast into 3D facial picture.

- *Automatic landmark identification.* One of the most promising fields is the automatic extraction of landmark coordinates. Currently, landmark assessment is a lengthy process that requires expert operators, and that may hinder a widespread use of 3D scans. The reliability of the data depends strongly on the operator's experience, because landmarks are usually located within relatively large and curves areas, rather than in correspondence of discrete points. Previous marking of the landmarks on the patient's skin reduces both the measurement error and the time required for image analysis, but even this process requires expertise and effort, and it may not be feasible for all subjects[100].

- *Individual identification for commercial, security, forensic and medical applications.*

- *Navigation system in surgery*

- *Geographical groups and human biology*

- *Aesthetic indices*

- *Craniofacial abnormalities.* 3D surface permits a better analysis of the facial configuration than that provided by a set of inter-landmark distances. One the most recent field of application is the biological analysis of statistical outliers that is of those abnormal/unusual morphologies that can derive from congenital or acquired malformations, traumas, or surgery. Quantitative assessment of facial phenotype may provide information to discover the root causes of disease with an unclear genetic background, like cleft lip with or without cleft palate[101]. Patients affected by craniofacial abnormalities necessitate several surgical procedure during the life: the use of methods and instruments that limit any additional burden to the patient is mandatory: repeated soft tissue

assessment are best performed by instruments that do not increase the radiation exposure of the children. Orthodontic and orthognathic surgery patients usually do not need the extensive treatments as provided to dysmorphic patients, but considering their number and their age, the use of diagnostic instruments with a reduced biological impact.

- *Facial aging*

- *Facial reconstruction in forensic and archaeological fields*

- *Manufacturing of objects and prostheses*

- *Archaeology*

3. CURRENT METHOD OF ASSESSING THE ACCURACY OF THREE-DIMENSIONAL SOFT TISSUE FACIAL PREDICTION: TECHNICAL AND CLINICAL CONSIDERATIONS

Since the introduction of three-dimensional (3D) imaging in orthognathic planning, there have been numerous studies reporting on the accuracy of facial soft tissue prediction of the various software systems. Determining the soft tissue accuracy of any 3D planning system is important, as it forms the basis of surgical or orthodontic plan and is only the visual aid available to show the patient their final predicted facial soft tissue appearance in 3D[102]. For analysis of 3D images, volumetric data – CT or CBCT- are generally converted into surface data prior to analysis; this is unnecessary for laser or sterophotogrammetry, as these techniques directly capture the air/soft tissue surface. These surface data can simply be thought of as hundreds if not thousands of 3D landmarks or points in space, joined together to form a 'polygonal surface mesh' or a 'triangular surface mesh'[103]. To date, several methods of analysis have been reported including: differences in distance of specific landmarks[104], differences between all the 3D points of the two entire facial surface meshes[105], and differences all 3D points of the two facial surface mesh following division into predefined anatomical regions[106].

Quantitative analysis of each technique involves measuring the linear distances between specific landmarks or between all the 3D points of the two 3D surfaces meshes. This can be performed taking into account the direction using the average distance difference, i.e. the signed difference, or irrespective of direction using the absolute Euclidean difference, and finally the root mean square (RMS) difference. The signed differences will cancel out positive and negative values, under-estimating the error; the absolute Euclidean difference will ignore the direction and only report the magnitude; and the RMS error will give disproportionate weight to very large differences. To reduce the effect of outlying points, the absolute distances between the numerous 3D points of the two surface meshes can be ordered in decreasing magnitude and the data within the 90th or 95th lower percentile can be averaged to produce the mean for the 90th or 95th percentile. The mean for the 90th

percentile can also be calculated using the same method. Other studies have reported the percentage of 3D points where the distance is 2 mm or less between the prediction and actual soft tissue surface meshes[107].

3.1 Analysis based on surface mesh

The analysis of 3D surface polygonal meshes is one method of assessing topographical and positional surface changes in 3D. Alignment can be made by superimposition of the hard tissues on the anterior cranial base; as the hard tissues relationship is 'locked', the distance between the two soft tissue surfaces can then be analysed. The second option is to ignore the underlying hard tissue and use the forehead region of the soft tissue only to align the two images. The results may be different, especially if the patient has lost adipose tissue from around the upper face region. Alignment of the images relying on the soft tissue only may also be difficult as there is less surface topography for the images to reliably align on.

Following alignment of the images, the distance between the two surface can be determined. The current method is based on the distance between one point on one surface and the closest point to it on the second surface. Note that the measurement relies on the closest point, which may not necessarily be the corresponding anatomical point. Unless the surface meshes are identical, there will be some points on one mesh where the closest point on the second mesh is absent, but the algorithm finds an inappropriate point on the second mesh and produces a large incorrect reading. To overcome the effects of this 'outliers', some studies 'filter-out' the values by using the 95^{th} and the 90^{th} percentiles. In the future it may be routine to use methods that rely on establishing 'anatomical correspondences' between the two independent images, such as dense correspondences and generic and conformed facial meshes[108].

As the facial surface mesh is made up of thousands of points, an overall mean value for the error is often reported. If one facial surface mesh is totally in front of the other, all the distance measurements will be either positive or negative and therefore the mean is valid. If however some parts of one mesh

lie behind and some in front of the other mesh, distance measurements for the whole face will be made up of positive and negative values. Any positive values will cancel out any negative values underestimating the mean difference and so biasing the results. In order to overcome this problem, some studies use the absolute mean values or Euclidean distances, which ignored the sign (direction) and report on the magnitude of error or the RMS error. The RMS error is derived from all the points making up the surface mesh, and a single numerical figure can in no way explain the accuracy of the prediction.

Many studies assess the accuracy of the prediction by comparing the differences in distance between the prediction and the actual surface using the entire face, including the areas that have been used for alignment. Therefore a large percentage of the mesh has minimal or no change; this will bias the accuracy by reducing the impact of the error – the data will be skewed towards the smaller values. In order to overcome this, areas of the face used for alignment can be excluded and the remaining mesh and the remaining mesh divided into anatomically relevant regions.

3.2 Analysis based on landmarks

The use of landmarks to assess soft tissue is routine practice in orthodontics; however this method greatly under-utilizes the 3D data. The positional changes of landmarks describe a change in an isolated point not a shape changes. The associate error of landmark identification will also add to the overall error of this method of analysis and can be over 2 mm depending on the landmark[109].

If landmarks are going to be used, the data need to be analysed correctly. If the direct difference of a landmark between two images is being measured, than the images need to be superimposed in order they are both aligned relative to the same 3D origin. If linear or angular measurements within each face are being analysed, this is not necessary. Another option is to select the same anatomical landmark on both meshes, extract the 3D coordinates of both points, and use software to calculate the Euclidean distance between the points. This required an extra step, but is clinically valid.

If the Euclidean distance is measured directly or indirectly, then only the magnitude of the error is known and the direction remains unknown. If the closest distance is used, than the mean will be calculated from the negative and positive data and will be underestimated. To overcome this problem the values can be recorded, the signs removed, and the average reading taken.

Khambay and Ullah[110] have proposed a protocol for future 3D imaging analysis that summarized these concepts (Table 2).

Process	**Method of assessment/report**
Generating prediction	Following alignment of the pre- and postoperative hard tissue images, use the postoperative hard tissue as a template to generate the soft tissue prediction
Registration of prediction and postoperative actual soft tissue	Report if superimposition was carried out on: (1) Hard tissue to hard tissue and analyse soft tissue surface difference (2) Soft tissue to soft tissue and analyse soft tissue surface difference
Method of analysis:	
(a) Surface mesh	Use specific anatomical regions to quantify the differences between the surfaces rather than complete facial surface mesh Use 95^{th} or 90^{th} percentile to eliminate outlying points Use absolute mean measurements (Euclidean) and standard deviations Introduce the use of anatomical correspondences between two images, i.e. dense correspondences masks or generic /conformed facial meshes
(b) Landmarks	Report on absolute mean measurements (Euclidean) and standard deviations. Measure the distance between corresponding anatomical landmarks on each mesh rather than the closest point.
(c) Curves	Further investigate the use of curves in analysis

Table 2. Protocol for three-dimensional analysis.

4. NATURAL HEAD POSITION

The natural position of the head (NHP) is the most balanced, natural position of the head when someone views an object at eye level. It is an individual, functional, physiological position that indicates a person's true appearance[111]. Since its introduction into orthodontics in the late 1950s it has been used as a reference position for the assessment of craniofacial morphology[112], and has been evocated as a better option than intracranial reference lines because it allegedly varies less. Measurements of the NHP is relevant in orthodontics for cephalometric analysis of dentofacial anomalies, orthognathic surgical planning, and evaluation of the relation between the head and the cervical column (craniocervical angulation). Cassi *et al*[113], in a recent review, have focused on techniques to establish it, and how to transfer it to the cephalostat, together with an overview of the 3-dimensional recording methods recently introduced into clinical practice. Numerous studies have successfully measured the reproducibility and stability of the NHP, both in short and long time-lapse[114,115,116]. Although NHP has less variability than intracranial reference lines, it is also influenced by balance (the vestibular canals of the middle ear), vision (the need to maintain a horizontal visual axis), and proprioception from joints and muscle involved in maintaining erect posture), so it depends on the subject's neuromuscular condition. In addition, it is not a single angular measurement, but a small range of angles oscillating around a mean posture[117], so is a dynamic concept which should be recorded both dynamically and continuously[118]. The protocol for obtaining the NHP seems to influence reproducibility, and there is some evidence that the success of a certain protocol depends on the operator[119]. The concept of 'estimated natural head position' or 'natural head orientation' was introduced because patients can have a habit of flexing or extending their head, and is defined as the orientation estimated by a trained clinical while the subjects stands with a relaxed body and head, and looks at a distant point at eye-level[120].

Natural head position can be calculated in two ways, the first of which uses the subject's own feeling of a natural head balance without external reference. The head position is the result of proprioceptive

information from muscles and ligaments and possibly from the utricular and semicircular canals, and the position is termed ‘self-balance’ position. The second method is based on visual cues from some external reference, as the subject positions the head so that they can observe either their eyes in the mirror (‘mirror’ position) or some device placed at a distance, horizontally, in front of the eyes. Positioning according to external reference should be done only after the head has been placed in the self-balanced position[121]. Both recordings are made with the teeth in occlusion. In adults the head is kept about 3° higher in the mirror position than in the self-balanced position.

Since the recent increase in interest in 3-dimensional imaging for orthodontic evaluation, several studies have been published that describe different ways to record natural head position[122,123].

Positioning of the head in cone-beam computed tomography is difficult because the scanning time is relatively long (20-40 s), which requires the patient’s head to be fixed to avoid movement. Hoogeveen *et al*[124] investigated whether the soft- tissue facial profile, as evaluated by soft-tissue cephalometric analysis, is different for a subject when in the natural or in supine head position, and they found no significant differences depending on the head position, except for the chin-throat angle, which is over 5° more acute when recorded supine, suggesting a more prominent chin. The authors advise that the picture of the chin-throat area should be accompanied by a complementary (photographic) recording in the natural head position.

There are two approaches: 1) 3-dimensional recording with the patient in the natural head position (placement of markers on patient’s face, digital orientation sensor or laser surface scanner), acquisition of the 3-dimensional image and subsequent reorientation of the volume according to the previously chosen natural head position; 2) ‘stereophotogrammetric natural head position’, a technique where the resulting facial surface image is recalibrated to correct orientation by using some physical references such as true vertical and mirror orientation[125]. Their first step is to record a digital mesh model of a hanging reference board placed at the capturing position of the stereophotogrammetry machine. The board is aligned to the vertical using a plumb bob, and to a laser plane parallel to a hanging mirror located at the centre of machine. The measurements derived from

the digital mesh model of the board are used to adjust the roll, pitch, and yaw of the subsequent facial images, and the physical reference information is valid until the next time that the machine is calibrated. This approach allows the patient to achieve the NHP without the use of any devices or troublesome markings on the face. It is extremely repeatable and accurate.

In a recent study, Zhu *et al*[126] determined the intra-rater and interrater reliability of reorientating three-dimensional (3D) facial images into the estimated natural head position. Three-dimensional facial images of 15 pre-surgical class III orthognathic patients were obtained and automatically re-orientated into natural head position (RNHP) using a 3d stereophotogrammetry system and in-hose software. Six clinicians were asked to estimate the NHP of these patients (ENHP); they re-estimated five randomly selected 3D images after 2-week interval. The differences in yaw, roll, pitch and chin position between RNHP and ENHP were measured. For intra-rater reliability, the intra-class correlation coefficient (ICC) values ranges from 0.55 to 0.77, representing moderate reliability for roll, yaw, pitch, and chin position, while for inter-rater reliability, the ICC values ranges from 0.38 to 0.58, indicating poor to moderate reliability. The median difference between ENHP and RNHP was small for roll and yaw, but larger for pitch. There was a tendency for the clinicians to estimate NHP with the chin tipped more posteriorly (6.3±5.2 mm) compared to RNHP, reducing the severity of the skeletal deformity in anterior-posterior direction.

Another interesting study was proposed by Hughes *et al*[127] to determine whether an observer's perception of the correct anatomical alignment of the head changes with time, and whether different observers agree on the correct anatomical alignment. To determine whether the perception of the correct anatomical alignment changes with time (intra-observer comparison), a group of 30 observers were asked to orient, into anatomical alignment, the three-dimensional (3D) head photograph of a normal man, on two separate occasions. To determine whether different observers agree on the correct anatomical alignment (inter-observer comparison), the observed orientations were compared. The results of intra-observer comparisons showed substantial variability between the first and second anatomical alignments. Bland-Altman coefficients of repeatability for pitch, yaw, and roll, were 6.9°,

4.4°, and 2.4°, respectively. The results of inter-observer comparisons showed that the agreement for roll was good (sample variance 0.4, standard deviation (SD) 0.7°), the agreement for yaw was moderate (sample variance 2.0, SD 1.4°), and the agreement for pitch was poor (sample variance 15.5, SD 3.9°). In conclusion, the perception of correct anatomical alignment changes considerably with time. Different observers disagree on the correct anatomical alignment. Agreement among multiple observers was bad for pitch, moderate for yaw, and good for roll.

Maal *et al*[128] have proposed a prospective study to determine variations in the face at rest; 100 3D photographs of the same individual were acquired at different times. Initially, 50 3D photographs were obtained; 25 using a wax bite to ensure similar occlusion between subsequent photographs and 25 without wax bite. This procedure was repeated 6 weeks later. Variation of the face at rest was computed. The influence of time and wax bite was investigated. Different anatomical regions were investigated separately. A mean variation of 0.25 mm (0.21-0.27 mm) was found (standard deviation 0.157 mm). No large differences were found between different time points or use of wax bite. Regarding separate anatomical regions, there were small variations in the nose and forehead regions; the largest variations were found in the mouth and eyes. This study showed small overall variation within the face at rest. In conclusion, different 3D photographs can be reproduced accurately and used in a clinical setting for treatment follow-up and evaluation.

5. PURPOSE OF THE STUDY

Anthropometric analysis of soft tissues is an integral part of orthodontic diagnosis and therapeutic planning. In the literature, various 3D imaging systems of soft facial tissues are described; currently the gold standard is represented by three-dimensional stereophothogrammetry. Each new stereophytogrammetric system requires a validation process that establishes accuracy and precision before clinical use, by identifying possible grinding and extrinsic errors to the system. The aim of this study is to validate the precision of a new 3D stereophotogrammetry system in terms of reliability, repeatability and reproducibility of the stereophotogrammetric image in the three planes of space.

Verifying any *in vivo* hypothesis necessarily presupposes a previous validation of the system *in vitro*, in terms of technical validation and knowledge of system errors in different acquisition conditions. To our best knowledge, no studies have been performed to investigate the accuracy of our stereophotogrammetric system in a clinical setting. This is precisely the first objective of this work.

After *in vitro* evaluation, the reproducibility and accuracy of the system *in vivo* has been investigated by analysing the variations of face anthropometric measurements between the reference position (NHP) and angular variations of pitch, roll and yaw movement of the head. There are no studies on soft tissue variations induced by head rotations in the three planes of space. This is the second objective of this work.

6. MATERIALS AND METHODS

6.1 Data acquisition

The scanner used is the Face Shape 3D Maxi Line Photogrammetric Scanner developed by Polishape 3D srl[129] (Bari, Italy). This photogrammetric system consists of six Canon EOS 1100D (12.2 megapixels) reflex cameras, mounted on a rigid support and positioned, two centrally and four laterally, on the support with a specific inclination. The lenses have a focal length of 50 mm.

To facilitate image capture and improve the surface texture quality, it is essential to obtain as much uniform light as possible on the surface of the face; for this reason, two external flashes are used as the only source of light in order to minimize the presence of light originated from other sources, whether natural or artificial (Fig. 6).

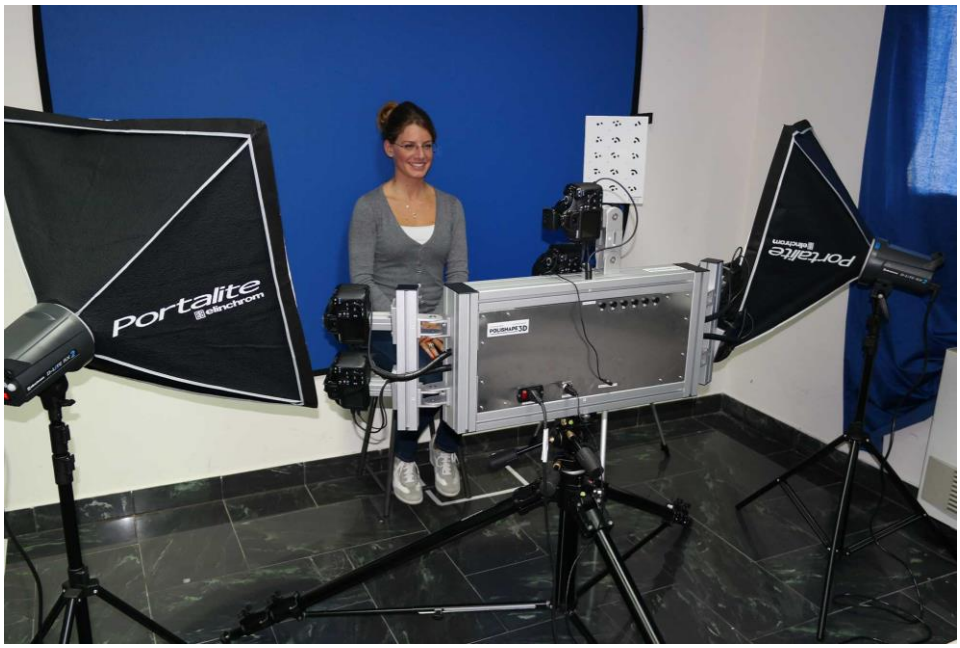

Figure 6. Face Shape 3D Maxi Line Photogrammetric Scanner

At a distance of one meter, a height-adjustable stool is placed so that the patient's eyes are positioned in front of the machine's lens positioned at the center of the support. Behind the subject is placed a monochrome panel to facilitate facial identification by the software.

The system is then connected to an external computer that controls the six cameras and receives the capture data from them. A previous work by Galantucci *et al*[130] have calibrated and examined the characteristics of this system by identifying an average system error of 0.425 mm as the variation compared to real measurements.

Calibration of the instrument can be done in two alternative ways:

- the first is a calibration that is performed before the patient shoots and consists of preventive stero-photogrammetric acquisition of a rectangular panel (Fig. 7) equipped with specific images that allows the software to calibrate and recognize the object's location in space. The advantage of this system is that the initial calibration is valid for all the subsequent shots made until the software is closed, while the disadvantage is that before you can make subsequent shots you have to wait for the system to process the image of the calibrator panel;

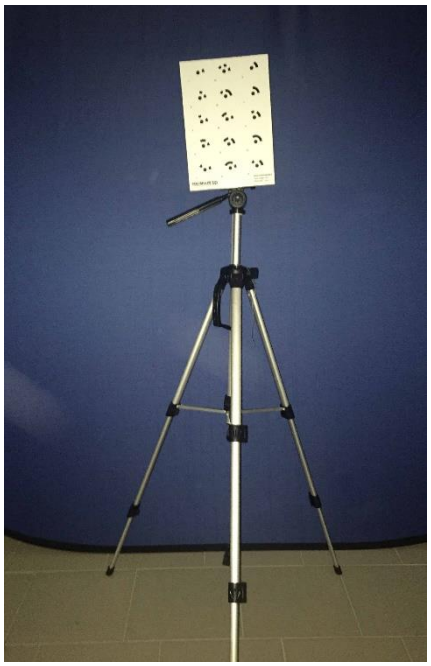

Figure 7. Calibrator panel.

- the second calibration is carried out using a collar which, worn by the subject (Fig. 8), will allow the contemporary calibration of the single shoot. The advantage of this technique is that you do not have to wait for calibration times with the panel, while the main disadvantage is

that the collar must be properly positioned to ensure that it is present in all six photographs for calibration to be successful.

Figure 8. Calibration collar.

In our study, we have chosen to use the second calibration system, which is more advantageous to our needs and, as indicated by the manufacturer, more accurate.

Using a remote control connected to the computer via USB, six simultaneous photographs are taken; synchronism is controlled by hardware and software. The images are then displayed on the computer as six separate shots and only then reworked to get a mesh that is a three-dimensional reconstruction of the face. 3D images thus created can be processed and analysed by various commercial software; the program was used in this study is Viewbox®.

Thanks to this software you can type on the mesh the anthropometric points corresponding to those previously marked on the dummy or the patient so that, by analyzing the coordinates *x*, *y*, *z* to identify the exact position.

6.2 Part I (in vitro)

In this study, we used the head of a dummy as a subject (Fig. 9), ideal for in vitro experimentation due to immobility and absence of facial mimicry. To improve image acquisition, the texture of the face was faded and opaque to reduce light reflection and, as suggested by the literature data[131], the following 23 anthropometric points were drawn with an eye-liner:

- 9 median: *Tragion* (Tr), *Glabella* (Gb), *Nasion* (N), *Pronasale* (Prn), *Subnasale* (Sn), *Labiale superius* (Ls), *Labiale inferius* (Li), *Sublabiale* (Sl), *Pogonion* (Pg);

- 7 bilateral: *Frontotemporalis* (Ft r/l), *Zygion* (Zy r/l), *Tragion* (Tr r/l), *Gonion* (Gn r/l), *Cheek* (Ch r/l), *Cheilion* (Chel r/l), *Orbitale inferius* (Or inf r/l).

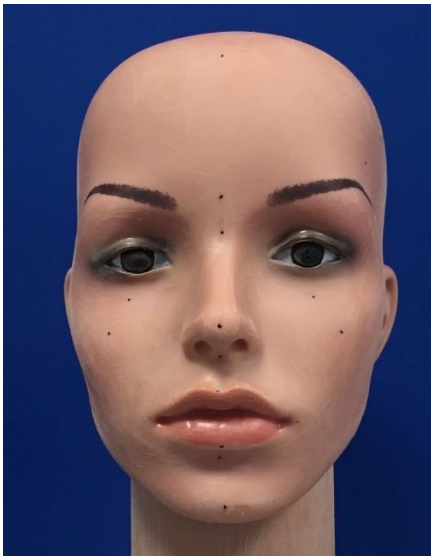

Figure 9. Dummy used in the study.

Finally, the dummy was placed on a support that allowed the head to be guided on the three planes of the space and equipped with a graduated scale to allow the acquisition of angular rotational values in the pitch, roll and yaw movements (Fig. 10).

Figure 10. Illustration of pitch (purple), roll (red) and yaw (yellow) movements.

To investigate the accuracy and repeatability of our system we chose to compare 50 shots of which:

- 10 with the head of the dummy not rotated in any direction (0 degrees), defined as reference position;

- 16 shots with the head of the dummy rotated in different degrees of yaw to the right and left (1,2,3,4,5,8,12,16 degrees);
- 32 shots with the head rotated at different degrees of pitches and rolls in both directions (1,2,3,4,5,7,9,11 degrees).

The shots were processed and the three-dimensional reconstructions obtained were the anthropometric points previously indicated on the dummy.

The shots were processed and the anthropometric points previously marked on the dummy were also marked on the three-dimensional reconstructions obtained. Their *x, y,* and *z* coordinates were collected from the software and saved in an Excel spreadsheed. 14 linear distances have been calculated:

- 4 median: *Chel$_{(r)}$-Chel$_{(l)}$; N-Prn; Sn-Pg; N-Pg*;
- 5 bilateral: *Glab-Ch$_{(r)}$; Glab-Ch$_{(l)}$; Glab-Ft$_{(r)}$; Glab-Ft$_{(l)}$; Zy$_{(l)}$-Tr$_{(l)}$; Zy$_{(r)}$-Tr$_{(r)}$; Ch$_{(r)}$-Tr$_{(r)}$; Ch$_{(l)}$-Tr$_{(l)}$;Ch$_{(r)}$-Gn$_{(r)}$; Ch$_{(l)}$-Gn$_{(l)}$.*

6.3 Part II (in vivo)

For *in vivo* validation, 10 volunteers recruited from dentistry students (5 males and 5 females) were used. Inclusion criteria were as follows:

- stable occlusion;
- no craniofacial or neuromuscular deformity,
- no history of facial trauma or plastic surgery intervention;
- no medications such as corticosteroids;
- good health and being in the healthy percentage of body mass index.

A single operator drew on each student's face the same anthropometric points used on the dummy, with an eye-liner, and in particular:

- 9 median: *Tragion* (Tr), *Glabella* (Gb), *Nasion* (N), *Pronasale* (Prn), *Subnasale* (Sn), *Labiale superius* (Ls), *Labiale inferius* (Li), *Sublabiale* (Sl), *Pogonion* (Pg);

- 7 bilateral: *Frontotemporalis* (Ft r/l), *Zygion* (Zy r/l), *Tragion* (Tr r/l), *Gonion* (Gn r/l), *Cheek* (Ch r/l), *Cheilion* (Chel r/l), *Orbitale inferius* (Or inf r/l).

During acquisition, special attention was addressed to positioning the volunteers and relaxing the facial musculature. The volunteer was so placed in NHP with the use of a mirror positioned in front of the patient's face.

The first acquisition was performed in NHP (five shots for each student at 15 seconds of distance) and this position was recorded as the reference position. Later, we asked each student to rotate the head on the three-floor space according to two progressive angles of 4 and 8 degrees relative to the reference position in both directions (left/right, high/low). Angle recording in pitch, roll, and yaw movements was performed using a head positioning laser system.

The shots were processed using Viewbox® and on each shot a single operator placed the anthropometric points previously plotted on the face surface; *x*, *y*, and *z* coordinates of these markings were exported to an Excel spreadsheet. Thus, 14 linear distances were calculated:

- 4 median: *$Chel_{(r)}$-$Chel_{(l)}$; N-Prn; Sn-Pg; N-Pg*;
- 5 bilateral: *Glab-$Ch_{(r)}$; Glab-$Ch_{(l)}$; Glab-$Ft_{(r)}$; Glab-$Ft_{(l)}$; $Zy_{(l)}$-$Tr_{(l)}$; $Zy_{(r)}$-$Tr_{(r)}$; $Ch_{(r)}$-$Tr_{(r)}$; $Ch_{(l)}$-$Tr_{(l)}$;$Ch_{(r)}$-$Gn_{(r)}$; $Ch_{(l)}$-$Gn_{(l)}$.*

6.4 Data processing and operational definitions

The distance between the points has been calculated as the square root of the sum of the differences in the three dimensions of the space, as indicated in the following formula:

$$d = \sqrt{\Delta x^2 + \Delta y^2 + \Delta z^2}$$

an analog to the *target registration error* (TRE) described in several literature articles[132,133].

The precision of the system has been divided into two subcategories:

1) Repeatability, defined as the degree of concordance between different measurements of the same object using the same technique. To analyse it we need to distinguish three different aspects:

- Operator error: it is highlighted by making different measurements of the same three-dimensional reconstruction performed by the same operator (intra-operator error) or by different operators (inter-operator error);
- Acquisition error: this is highlighted when multiple shots and more 3D reconstructions of the same object occur;
- Recording error: that is due to different calibrations of the machine that take place between one shot and the other.

2) Reproducibility, defined as the degree of concordance between measurements made by two different operators using the same technique on the same subject.

To investigate operator error we used a single click at 0 degrees and the same relative three-dimensional processing; the anthropometric points were then positioned 10 times by the same operator (intra-operator error) and five times by two different operators (inter-operator error).

In order to investigate the acquisition error, five different shots were compared with the subject always in the same position (0 degrees), and the points were positioned by the same operator.

The recording error was minimized by using the calibration collar at every shot.

To investigate the reproducibility of the system, two different operators typed the points on different elaborations of different shots made with the dummy positioned at 0 degrees.

6.5 Data analysis

The data obtained were processed both in terms of descriptive statistics (mean, standard deviation, standard error, variation coefficient, maximum and minimum value, and ranges calculated for all series of measurements) and in terms of inferential statistics. The difference between the

measurements were calculated and summarized. The goal was to estimate the system error in the various conditions of acquisition. Particular attention has been paid to the analysis of intraoperator, interoperator and capture errors calculated in terms of average error, maximum error, standard error, standard deviation and variation coefficient. The analysis was performed using Microsoft Excel and free software for epidemiology Winpepi[134].

When a constant physical magnitude is measured with an apparatus where both statistical and systematic errors are present, repeated measurements provide obviously different values. From a sample of N measurements, computed the mean (M) and the standard deviation (SD), the uncertainty of the sample measurement observed is given by the sum of two variables, one related to statistical error, in terms of standard error, and one linked to systematic error, in terms of maximum error. For these reasons, the measurements were reported with the following formula:

$$x = m \pm \frac{s}{\sqrt{N}}\,(\text{stat}) \pm \frac{\Delta}{2}\,(\text{syst})$$

The stability of the measurements carried out in different conditions (for example obtained with the dummy in the reference position and with different degrees of inclination) was verified by establishing a threshold value as a statistical significance limit, taking into account the intrinsic variability of the system in terms of reproducibility error of the system previously calculated under constant conditions (reference position). The null hypothesis was that there is no substantial difference between the measurements in different condition both *in vivo* and *in vitro*.

The statistical analysis was performed with Winpepi and the test used is the Westlake-Schuirmann equivalence test (which is part of the *t*-tests) with $p < 0.05$, so the mean equivalence of two sets of measurements is defined as a difference not higher than the maximum error of the system calculated previously.

The Student's t-test and ANOVA are statistical test for 'zero difference' hypothesis; if we want to determine equivalence, a more appropriate statistical question to ask is if there is an unacceptable

difference between two sets of measurements. The Westlake Interval can be used to determine equivalence; Shuirmann's Two One-side test is an alternative equivalence test. It is different from the Student *t*-test because does not assume there is no difference in the result. If one wants to that the distribution of results is within an acceptable difference, this test can be used.

The test was repeated for each set of measurements detected with the dummy in reference position and with different degrees of rotation; a comparison was made between all the series of measurements obtained for the individual rotation types (pitch, roll, and yaw) in order to establish any statistical equivalence with the measurements obtained with multiple shots at 0 degrees. Comparisons were also made within each set of measurements, for example by contrasting the values measured with low rotation degrees to those obtained with higher degrees, or by comparing two different directions of rotation to record any statistically significant differences.

7. RESULTS

7.1 Part I (in vitro) - Operator error

Intra-operator error as an error resulting from inaccuracies in placing the landmarks by one operator was assessed by 10 redigitizing anthropometric points on the same three-dimensional reconstruction of the dummy in the reference position.

The table below (Table 3) contains the descriptive statistic of the intraoperative error in terms of mean, standard deviation, standard error, confidence intervals, variation coefficient and minimum/maximum value.

INTRAOPERATORE	media	dev.st	err.st	CI95%Low	CI95%High	min	max	CV	d_min	d_max	errore_m
Chel(r)-Chel(l)	54,629	0,133	0,042	54,513	54,746	54,447	54,908	0,243	-0,183	0,279	0,231
N-Pronasale	42,942	0,188	0,059	42,777	43,107	42,629	43,297	0,437	-0,313	0,355	0,334
Sn-Pg	56,680	0,124	0,039	56,571	56,789	56,431	56,830	0,219	-0,249	0,151	0,200
N-Pg	105,608	0,257	0,081	105,382	105,834	105,221	105,893	0,244	-0,387	0,285	0,336
Glab-Ch(r)	67,596	0,135	0,043	67,477	67,714	67,316	67,788	0,200	-0,280	0,192	0,236
Glab-Ch(l)	67,945	0,125	0,040	67,835	68,055	67,738	68,158	0,184	-0,207	0,213	0,210
Glab-Ft(r)	65,607	0,107	0,034	65,512	65,701	65,413	65,823	0,163	-0,194	0,216	0,205
Glab-Ft(l)	65,376	0,071	0,023	65,313	65,439	65,261	65,506	0,109	-0,115	0,131	0,123
Zy(l)-Tr(l)	29,252	0,096	0,030	29,167	29,337	29,134	29,411	0,330	-0,118	0,159	0,138
Zy(r)-Tr(r)	30,729	0,149	0,047	30,598	30,860	30,439	30,924	0,486	-0,290	0,195	0,242
Ch(r)-Tr(r)	82,389	0,112	0,035	82,291	82,488	82,177	82,529	0,136	-0,212	0,139	0,176
Ch(l)-Tr(l)	82,344	0,114	0,036	82,244	82,445	82,112	82,508	0,139	-0,232	0,164	0,198
Ch(r)-Gn(r)	53,938	0,092	0,029	53,857	54,019	53,853	54,158	0,171	-0,085	0,220	0,153
Ch(l)-Gn(l)	51,968	0,097	0,031	51,883	52,054	51,857	52,136	0,187	-0,111	0,168	0,139

Table 3. Descriptive statistics of intra-operator error.

Standard errors mean is 0.041 mm, with a minimum value of 0.023 mm in the *Glabella-Frontotemporal*(l) measurement and a maximum value of 0.081 mm in the *Nasion-Pogonion* measurement. The latter has the highest maximum error (0.336 mm) (Fig. 11).

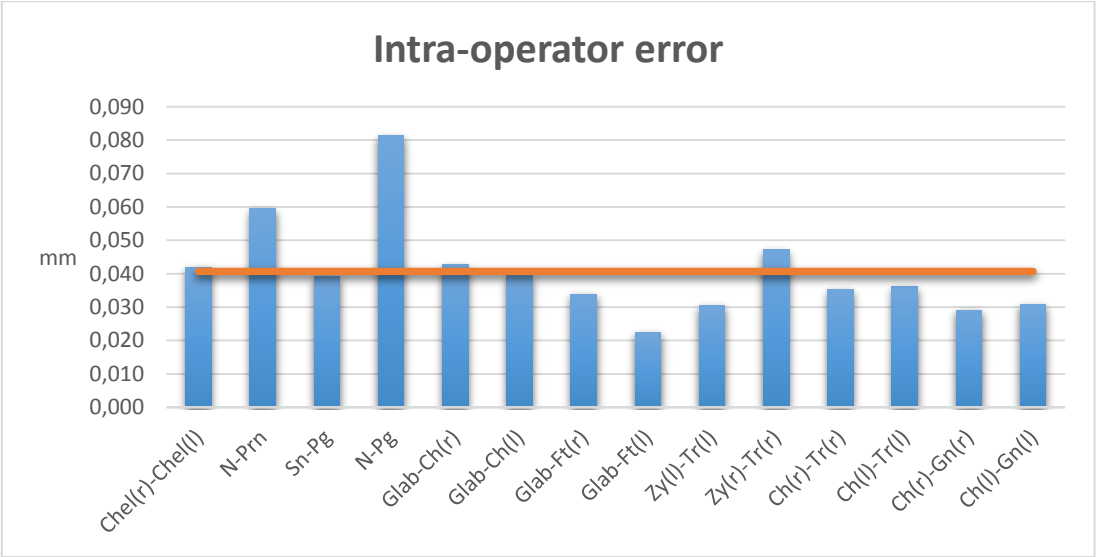

Figure 11. Standard intra-operator error.

Inter operator error is an error resulting from inaccuracies in placing the landmarks by two operators, It was assessed by redigitizing anthropometric points on the same three-dimensional reconstruction of the dummy in the reference position (5 times by one operator and 5 times by the other operator) (Table 4).

INTEROPERATORE	media	dev.st	err.st	CI95%Low	CI95%High	min	max	CV	d_min	d_max	errore_m
Chel(r)-Chel(l)	54,711	0,165	0,052	54,566	54,856	54,498	55,013	0,301	-0,213	0,302	0,257
N-Pronasale	42,738	0,265	0,084	42,505	42,970	42,379	43,065	0,620	-0,358	0,327	0,343
Sn-Pg	56,727	0,227	0,072	56,528	56,926	56,431	57,254	0,400	-0,297	0,526	0,411
N-Pg	105,363	0,351	0,111	105,055	105,672	104,828	105,893	0,333	-0,535	0,530	0,532
Glab-Ch(r)	67,615	0,170	0,054	67,466	67,764	67,316	67,833	0,251	-0,299	0,218	0,258
Glab-Ch(l)	68,086	0,234	0,074	67,881	68,292	67,813	68,560	0,343	-0,274	0,474	0,374
Glab-Ft(r)	65,608	0,147	0,046	65,479	65,737	65,388	65,835	0,224	-0,219	0,227	0,223
Glab-Ft(l)	65,451	0,153	0,048	65,317	65,586	65,216	65,707	0,234	-0,235	0,256	0,246
Zy(l)-Tr(l)	29,196	0,197	0,062	29,023	29,368	28,866	29,438	0,673	-0,330	0,242	0,286
Zy(r)-Tr(r)	30,842	0,258	0,082	30,616	31,069	30,439	31,249	0,836	-0,404	0,406	0,405
Ch(r)-Tr(r)	82,508	0,217	0,068	82,318	82,698	82,177	82,949	0,262	-0,331	0,441	0,386
Ch(l)-Tr(l)	82,350	0,167	0,053	82,203	82,496	82,112	82,718	0,203	-0,238	0,368	0,303
Ch(r)-Gn(r)	53,945	0,127	0,040	53,833	54,057	53,718	54,158	0,236	-0,227	0,213	0,220
Ch(l)-Gn(l)	51,993	0,154	0,049	51,858	52,128	51,731	52,194	0,296	-0,262	0,200	0,231

Table 4. Descriptive statistics of inter-operator error.

The standard inter-operator error was higher than the intra-operator value with a mean value of 0.064 mm, a minimum value of 0.04 mm in the *Chelion-Gonion* (r) measurement and a maximum value of 0.111 mm in the *Nasion-Pogonion* measurement whose error maximum was found to be 0.532 mm (Fig. 12).

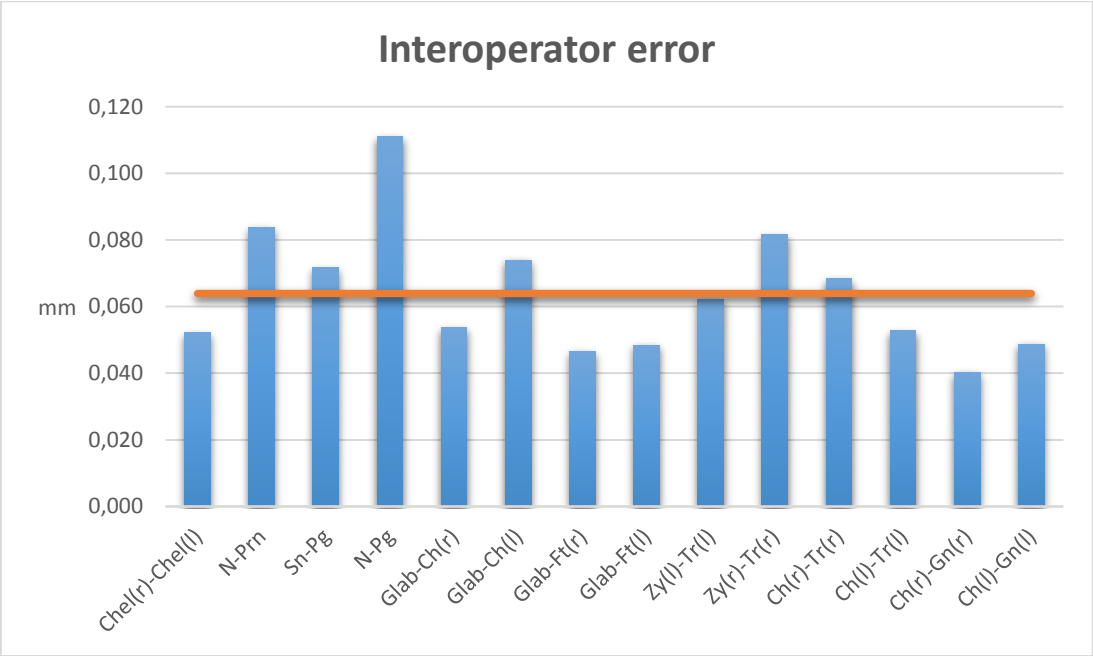

Figure 12. Standard inter-operator error.

7.2 Acquisition error

Acquisition error is an error resulting from different three-dimensional image captures of the same object on which anthropometric points are typed by a single operator (Table 5).

ACQUISIZIONE 1	media	dev.st	err.st	CI95%Low	CI95%High	min	max	CV	d_min	d_max	errore_m
Chel(r)-Chel(l)	54,990	0,187	0,084	54,758	55,223	54,782	55,288	0,340	-0,208	0,298	0,253
N-Pronasale	42,588	0,293	0,131	42,224	42,952	42,182	42,912	0,688	-0,406	0,324	0,365
Sn-Pg	56,742	0,216	0,097	56,473	57,010	56,500	57,019	0,381	-0,242	0,277	0,259
N-Pg	105,123	0,236	0,105	104,831	105,416	104,837	105,397	0,224	-0,286	0,274	0,280
Glab-Ch(r)	67,747	0,229	0,102	67,463	68,031	67,414	68,042	0,338	-0,333	0,295	0,314
Glab-Ch(l)	68,075	0,174	0,078	67,858	68,291	67,924	68,283	0,256	-0,151	0,208	0,179
Glab-Ft(r)	65,674	0,148	0,066	65,491	65,857	65,524	65,883	0,225	-0,150	0,209	0,179
Glab-Ft(l)	65,490	0,183	0,082	65,263	65,718	65,248	65,676	0,280	-0,242	0,186	0,214
Zy(l)-Tr(l)	29,237	0,188	0,084	29,004	29,471	29,016	29,507	0,643	-0,221	0,270	0,246
Zy(r)-Tr(r)	30,857	0,396	0,177	30,366	31,349	30,457	31,377	1,283	-0,400	0,520	0,460
Ch(r)-Tr(r)	82,504	0,247	0,110	82,198	82,811	82,202	82,774	0,299	-0,302	0,270	0,286
Ch(l)-Tr(l)	82,427	0,363	0,162	81,976	82,877	81,848	82,839	0,440	-0,579	0,412	0,496
Ch(r)-Gn(r)	51,868	0,232	0,104	51,580	52,156	51,673	52,151	0,447	-0,195	0,283	0,239
Ch(l)-Gn(l)	53,954	0,121	0,054	53,804	54,104	53,803	54,133	0,224	-0,151	0,179	0,165

Table 5. Descriptive statistics of acquisition error.

Mean standard error is 0.103 mm with a minimum value of 0.066 mm for *Glabella-Frontotemporale* (r) and a maximum value of 0.177 mm for *Zygion*(r)-*Tragion*(r). The highest maximum error was found in the *Cheek*(l)-*Tragion* (l) measurement of 0.496 mm (Fig. 13).

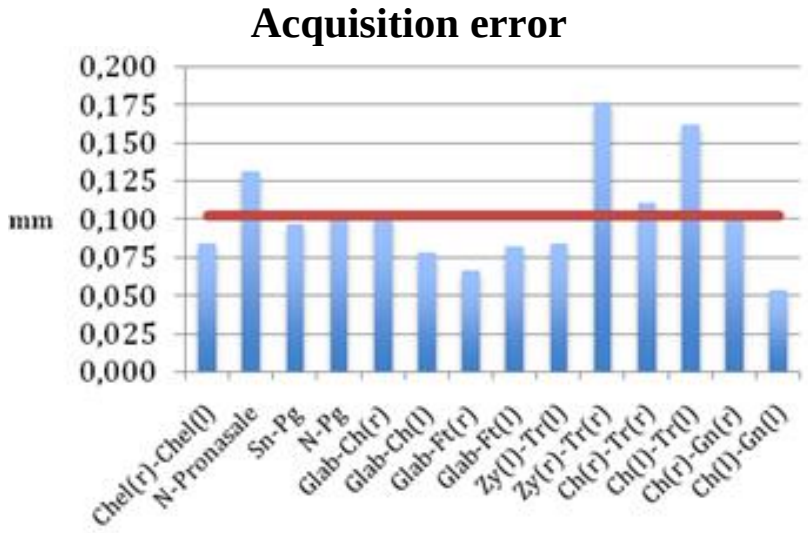

Figure 13. Standard error acquisition.

7.3 Reproducibility error

Reproducibility error is an error resulting from different three-dimensional image captures of the same object on which anthropometric points are typed by two operators (Tab. 6). It represents the overall variability of the system, as it encompasses all the variables previously examined.

RIPRODUCIBILITA'	media	dev.st	err.st	CI95%Low	CI95%High	min	max	CV	d_min	d_max	errore_m
Chel(r)-Chel(l)	54,786	0,334	0,106	54,492	55,079	54,218	55,288	0,610	-0,567	0,502	0,535
N-Pronasale	42,646	0,310	0,098	42,373	42,918	42,182	43,285	0,728	-0,464	0,639	0,551
Sn-Pg	56,795	0,218	0,069	56,603	56,987	56,500	57,197	0,384	-0,295	0,402	0,349
N-Pg	105,261	0,275	0,087	105,019	105,502	104,837	105,684	0,261	-0,424	0,423	0,423
Glab-Ch(r)	67,655	0,189	0,060	67,489	67,820	67,414	68,042	0,279	-0,241	0,387	0,314
Glab-Ch(l)	68,145	0,252	0,080	67,924	68,366	67,843	68,644	0,370	-0,302	0,499	0,401
Glab-Ft(r)	65,662	0,102	0,032	65,572	65,751	65,524	65,883	0,155	-0,138	0,221	0,179
Glab-Ft(l)	65,508	0,160	0,051	65,367	65,648	65,248	65,691	0,245	-0,260	0,183	0,221
Zy(l)-Tr(l)	29,093	0,259	0,082	28,865	29,320	28,633	29,507	0,891	-0,460	0,415	0,437
Zy(r)-Tr(r)	30,993	0,413	0,131	30,630	31,356	30,457	31,696	1,333	-0,536	0,703	0,620
Ch(r)-Tr(r)	82,671	0,404	0,128	82,317	83,025	82,202	83,558	0,488	-0,469	0,887	0,678
Ch(l)-Tr(l)	82,234	0,520	0,164	81,777	82,690	81,059	82,839	0,632	-1,175	0,605	0,890
Ch(r)-Gn(r)	51,930	0,220	0,069	51,737	52,123	51,673	52,326	0,423	-0,257	0,396	0,326
Ch(l)-Gn(l)	53,960	0,147	0,047	53,831	54,089	53,763	54,236	0,273	-0,197	0,276	0,236

Table 6. Descriptive statistic of reprodubility error.

Mean standard error was 0.086 mm with a distribution of values between 0.032 mm for *Glabella*-*Frontotemporale*(l) and 0.164 mm for *Cheek*(l)-*Tragion*(l). The latter is also characterized by the largest value of the maximum recorded error of 0.890 mm (Fig. 14).

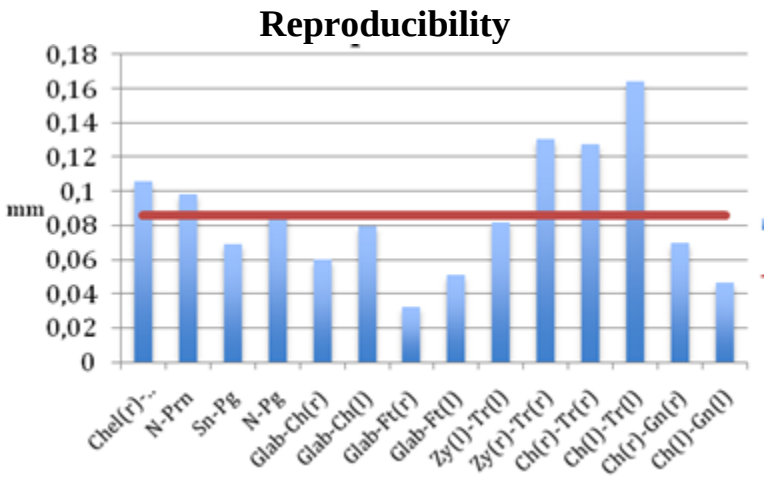

Figura 14. Standard reproducibility error.

From the overall analysis of the results obtained in the reference position, it was possible to calculate a maximum intra-operator error which, as suspected, was the smallest (0.336 mm) as it contains only one variable, the operator itself. The second smallest error (0.496 mm) is found in the acquisition error, where the previous error adds to the intrinsic error of the machine performing repeated shots under the same conditions. If the variable of a second operator (inter-operator error) is added, the maximum error increases further reaching a value of 0.532 mm suggesting that the "operator" variable plays a greater role in increasing the variability of the results. The last analysis in the 0-degree position was the search of the reproducibility error, which by definition contains all the previous errors. As expected, the maximum error was greater than the previous (0.890 mm), thus representing the overall system error, that is, the maximum uncertainty of our measurements (Fig.15,16).

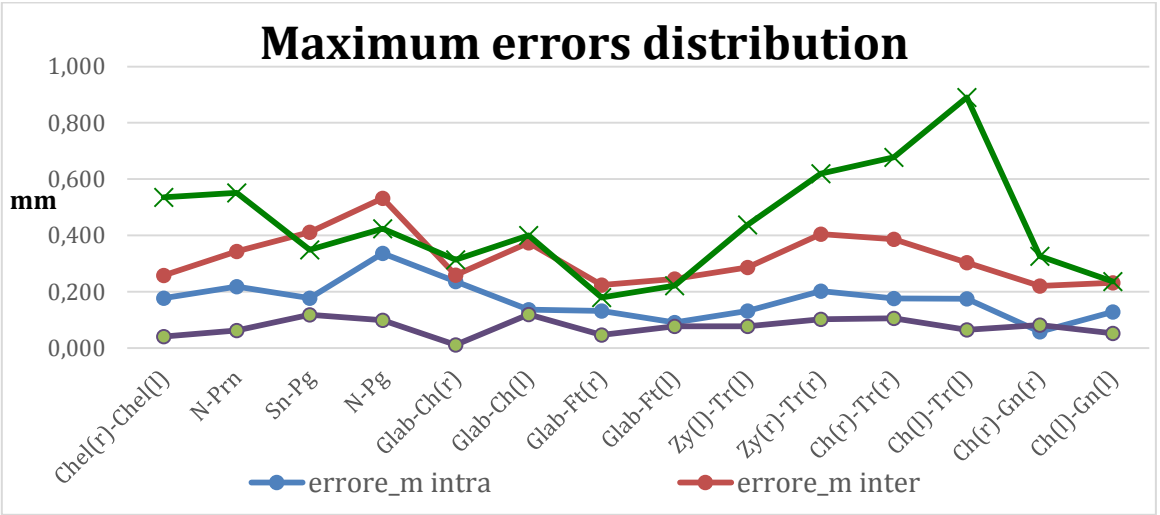

Figure 15. Maximum error distribution.

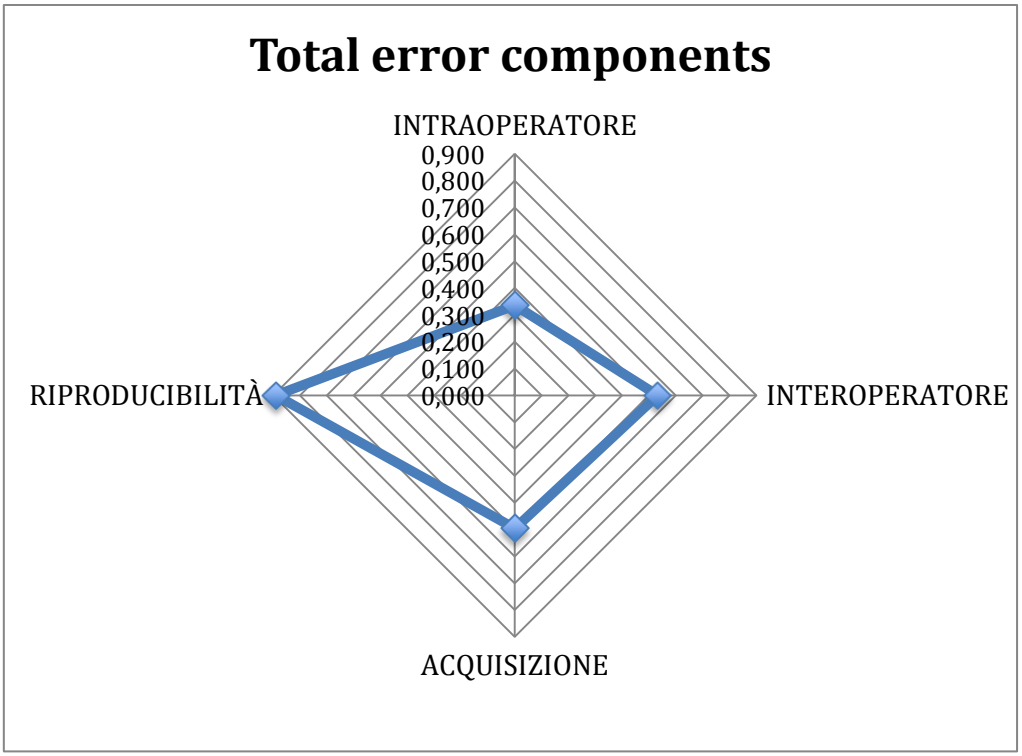

Figure 16. Total error components.

7.4 Error analysis and rotations equivalence

After identifying the errors and the maximum variability of our measurements, the focus was on assessing the influence of rotations on the accuracy of these measurements. The equivalence limit is represented by the maximum error of the measured system at the reference point (0.89 mm), in order to highlight statistically significant differences in the measurements between anthropometric points in the different acquisition conditions.

Yaw

Table 7 shows the comparison between the linear anthropometric values between reference position and progressive angular values of yaw (movement to the right and to the left).

IMBARDATA VS. FISSO	media	dev.st	err.st	min	max	CV	CI95%Low	CI95%High	d_min	d_max	errore_m	m.imbardat	m.fisso	sd_imbard	sd_fisso	p-value (A>B)	p-value (B>A)
Chel(r)-Chel(l)	54,691	0,354	0,084	53,982	55,288	0,648	52,183	55,781	-0,709	0,597	0,653	54,534	54,849	0,361	0,284	0,000	0,020
N-Pronasale	42,605	0,267	0,063	42,182	43,285	0,626	40,443	43,921	-0,423	0,680	0,551	42,564	42,646	0,198	0,329	0,000	0,000
Sn-Pg	56,868	0,237	0,056	56,500	57,376	0,417	55,341	57,659	-0,368	0,508	0,438	56,944	56,792	0,231	0,231	0,000	0,000
N-Pg	105,308	0,260	0,061	104,837	105,766	0,247	104,152	105,522	-0,471	0,458	0,465	105,371	105,246	0,229	0,287	0,000	0,000
Glab-Ch(r)	67,644	0,185	0,044	67,287	68,042	0,273	66,529	68,045	-0,357	0,398	0,377	67,613	67,675	0,186	0,188	0,000	0,000
Glab-Ch(l)	68,312	0,322	0,076	67,843	68,858	0,471	66,534	69,152	-0,468	0,547	0,508	68,491	68,132	0,280	0,264	0,006	0,000
Glab-Ft(r)	65,653	0,095	0,022	65,520	65,883	0,145	65,118	65,922	-0,133	0,230	0,182	65,641	65,664	0,086	0,108	0,000	0,000
Glab-Ft(l)	65,601	0,207	0,049	65,248	65,910	0,315	64,373	66,123	-0,353	0,309	0,331	65,685	65,518	0,217	0,167	0,006	0,016
Zy(l)-Tr(l)	28,972	0,401	0,094	28,107	29,691	1,383	24,267	31,947	-0,865	0,719	0,792	28,800	29,144	0,478	0,215	0,000	0,012
Zy(r)-Tr(r)	30,965	0,452	0,107	30,115	31,696	1,461	26,059	34,171	-0,850	0,731	0,791	30,969	30,961	0,504	0,425	0,004	0,004
Ch(r)-Tr(r)	82,730	0,383	0,090	82,202	83,558	0,462	80,918	83,486	-0,528	0,828	0,678	82,887	82,572	0,426	0,272	0,033	0,001
Ch(l)-Tr(l)	82,154	0,442	0,104	81,059	82,839	0,538	79,565	82,553	-1,095	0,685	0,890	81,943	82,364	0,450	0,335	0,000	0,009
Ch(l)-Gn(l)	53,961	0,165	0,039	53,681	54,283	0,306	52,831	54,531	-0,280	0,322	0,301	53,941	53,982	0,195	0,138	0,000	0,000
Ch(r)-Gn(r)	51,923	0,242	0,057	51,389	52,326	0,465	50,097	52,681	-0,533	0,404	0,468	51,959	51,886	0,298	0,180	0,000	0,000

Table 7. Comparison of measurements obtained at different yaw degrees with those obtained with the shots at 0 degrees: mean, standard deviation (dev.st), standard error (err.st); lower 95% confidence interval (CI95% Low), high 95% confidence interval (CI95% high), minimum value (min), maximum value (max), variation coefficient (CV), difference between minimum and mean value (d_min), difference between minimum and mean value (d_min), maximum error (error_m).

As shown in the table, the two sets of measurements were found to be significantly equivalent (p <0.01). A mean difference of 0.422 mm was found in the *Cheek*(l)-*Tragion*(l) distance comparison. The same evaluation was carried out to find out the existence of any differences between the low and the high grades. There were no significant differences even from the comparison between high and low rotation degrees. The maximum difference was found for *Zygion*(r)-*Tragion* (r) of 0.455 mm.

Roll

Subsequently, the roll data was compared with the measurements in the reference position (0 degrees) (Tab. 8).

ROLLIO SXvsFISSO	media	dev.st	err.st	min	max	CV	CI95%Low	CI95%High	d_min	d_max	errore_m	media fisso	media rollio	sd_fisso	sd_rollio	p-value (A>B)	p-value (B>A)
Chel(r)-Chel(l)	54,882	0,221	0,054	54,278	55,288	0,403	53,158	55,398	-0,604	0,406	0,505	54,849	54,919	0,284	0,129	0,000	0,000
N-Pronasale	42,820	0,346	0,084	42,182	43,504	0,807	39,941	44,423	-0,638	0,684	0,661	42,646	43,016	0,329	0,258	0,000	0,032
Sn-Pg	56,783	0,204	0,049	56,500	57,197	0,359	55,504	57,496	-0,283	0,414	0,349	56,792	56,773	0,231	0,183	0,000	0,000
N-Pg	105,187	0,305	0,074	104,801	105,735	0,290	103,996	105,605	-0,386	0,548	0,467	105,246	105,120	0,287	0,329	0,001	0,000
Glab-Ch(r)	67,704	0,230	0,056	67,231	68,229	0,339	66,289	68,172	-0,473	0,525	0,499	67,675	67,736	0,188	0,279	0,000	0,000
Glab-Ch(l)	68,062	0,269	0,065	67,589	68,644	0,396	66,490	68,688	-0,473	0,582	0,527	68,132	67,983	0,264	0,270	0,000	0,000
Glab-Ft(r)	65,689	0,146	0,035	65,383	65,888	0,222	64,768	65,998	-0,306	0,199	0,252	65,664	65,716	0,108	0,183	0,000	0,000
Glab-Ft(l)	65,325	0,303	0,073	64,800	65,691	0,463	63,514	66,086	-0,525	0,366	0,446	65,518	65,108	0,167	0,276	0,020	0,000
Zy(l)-Tr(l)	28,888	0,338	0,082	28,379	29,507	1,172	25,126	31,632	-0,509	0,619	0,564	29,144	28,600	0,215	0,174	0,009	0,000
Zy(r)-Tr(r)	30,813	0,461	0,112	29,767	31,696	1,498	25,609	33,925	-1,046	0,883	0,964	30,961	30,647	0,425	0,470	0,008	0,000
Ch(r)-Tr(r)	82,578	0,315	0,076	82,003	83,077	0,381	80,944	83,062	-0,575	0,499	0,537	82,572	82,584	0,272	0,377	0,000	0,000
Ch(l)-Tr(l)	82,169	0,354	0,086	81,540	82,839	0,431	80,345	82,736	-0,628	0,670	0,649	82,364	81,949	0,335	0,231	0,001	0,000
Ch(r)-Gn(r)	54,012	0,340	0,082	53,010	54,498	0,630	51,262	54,758	-1,002	0,486	0,744	53,982	54,045	0,138	0,490	0,000	0,002
Ch(l)-Gn(l)	51,937	0,157	0,038	51,673	52,193	0,302	50,835	52,511	-0,264	0,256	0,260	51,886	51,994	0,180	0,109	0,000	0,000

Table 8. Comparison of the measurements obtained from shots at 0 degrees with those obtained at different degrees of roll to the left: mean, standard deviation (dev.st), standard error (err.st); lower 95% confidence interval (CI95% Low), high 95% confidence interval (CI95% high), minimum value (min), maximum value (max), variation coefficient (CV), difference between minimum and mean value (d_min), difference between minimum and mean value (d_min), maximum error (error_m).

The two series of measurements were found to be significantly equivalent ($p < 0.01$). The maximum difference between the averages was 0.543 mm calculated for *Zygion*(l)-*Tragion*(l). As before, the low and high rotation degrees were compared. In Tables 9 we can see how even in this case the

measurements were significantly equivalent with a maximum difference between the 0.41 mm averages in the *Zygion*(r)-*Tragion*(r).

ROLLIO	media	dev.st	err.st	CI95%Low	CI95%High	min	max	CV	d_min	d_max	errore_m	media bassa	media alta	sd-bassa	sd_alta	p-value (A>B)	p-value (B>A)
Chel(r)-Chel(l)	54,871	0,157	0,039	54,762	54,980	54,538	55,094	0,286	-0,333	0,224	0,278	54,840	54,902	0,204	0,095	0,000	0,000
N-Pronasale	42,968	0,241	0,060	42,801	43,136	42,412	43,504	0,562	-0,556	0,536	0,546	42,958	42,978	0,316	0,157	0,000	0,000
Sn-Pg	56,693	0,173	0,043	56,573	56,814	56,347	57,076	0,305	-0,346	0,383	0,365	56,732	56,655	0,142	0,201	0,000	0,000
N-Pg	105,027	0,272	0,068	104,838	105,216	104,674	105,735	0,259	-0,353	0,708	0,531	105,037	105,016	0,259	0,302	0,000	0,000
Glab-Ch(r)	67,699	0,278	0,069	67,506	67,892	67,119	68,229	0,410	-0,580	0,530	0,555	67,539	67,859	0,268	0,186	0,000	0,005
Glab-Ch(l)	68,013	0,211	0,053	67,867	68,160	67,589	68,537	0,311	-0,424	0,524	0,474	67,975	68,052	0,197	0,232	0,000	0,000
Glab-Ft(r)	65,729	0,153	0,038	65,623	65,835	65,383	65,897	0,233	-0,346	0,168	0,257	65,723	65,735	0,140	0,175	0,000	0,000
Glab-Ft(l)	65,125	0,254	0,064	64,948	65,302	64,585	65,545	0,391	-0,540	0,420	0,480	65,272	64,978	0,179	0,239	0,002	0,000
Zy(l)-Tr(l)	28,648	0,243	0,061	28,479	28,817	28,379	29,296	0,850	-0,269	0,648	0,459	28,775	28,522	0,274	0,124	0,001	0,000
Zy(r)-Tr(r)	30,602	0,422	0,106	30,309	30,895	29,643	31,259	1,380	-0,959	0,657	0,808	30,807	30,397	0,265	0,465	0,010	0,000
Ch(r)-Tr(r)	82,489	0,404	0,101	82,209	82,770	81,633	83,077	0,490	-0,856	0,588	0,722	82,617	82,362	0,389	0,402	0,031	0,000
Ch(l)-Tr(l)	81,869	0,284	0,071	81,672	82,067	81,464	82,366	0,347	-0,405	0,497	0,451	82,052	81,687	0,221	0,220	0,009	0,000
Ch(r)-Gn(r)	54,065	0,350	0,087	53,822	54,307	53,010	54,498	0,647	-1,055	0,433	0,744	54,180	53,949	0,233	0,421	0,012	0,000
Ch(l)-Gn(l)	52,015	0,153	0,038	51,909	52,121	51,644	52,267	0,294	-0,370	0,252	0,311	52,041	51,989	0,199	0,094	0,000	0,000

Table 9. Comparison of measurements obtained in low and high rolling grades: mean, standard deviation (dev.st), standard error (err.st); lower 95% confidence interval (CI95% Low), high 95% confidence interval (CI95% high), minimum value (min), maximum value (max), variation coefficient (CV), difference between minimum and mean value (d_min), difference between minimum and mean value (d_min), maximum error (error_m).

In addition, the comparison between the two directions was performed (Table 10) and even in this case the two sample measurements were equivalent ($p < 0.05$) with a maximum difference between the averages in *Cheek*(r)-*Tragion*(r) of 0.189 mm.

ROLLIO	media	dev.st	err.st	CI95%Low	CI95%High	min	max	CV	d_min	d_max	errore_m	medi_destra	media_sinistra	sd_destra	sd_sinistra	p-value (A>B)	p-value (B>A)
Chel(r)-Chel(l)	54,871	0,157	0,039	54,762	54,980	54,538	55,094	0,286	-0,333	0,224	0,278	54,823	54,919	0,176	0,129	0,000	0,000
N-Pronasale	42,968	0,241	0,060	42,801	43,136	42,412	43,504	0,562	-0,556	0,536	0,546	42,921	43,016	0,231	0,258	0,000	0,000
Sn-Pg	56,693	0,173	0,043	56,573	56,814	56,347	57,076	0,305	-0,346	0,383	0,365	56,614	56,773	0,127	0,183	0,000	0,000
N-Pg	105,027	0,272	0,068	104,838	105,216	104,674	105,735	0,259	-0,353	0,708	0,531	104,934	105,120	0,174	0,329	0,000	0,001
Glab-Ch(r)	67,699	0,278	0,069	67,506	67,892	67,119	68,229	0,410	-0,580	0,530	0,555	67,662	67,736	0,291	0,279	0,000	0,000
Glab-Ch(l)	68,013	0,211	0,053	67,867	68,160	67,589	68,537	0,311	-0,424	0,524	0,474	68,043	67,983	0,144	0,270	0,000	0,000
Glab-Ft(r)	65,729	0,153	0,038	65,623	65,835	65,383	65,897	0,233	-0,346	0,168	0,257	65,741	65,716	0,128	0,183	0,000	0,000
Glab-Ft(l)	65,125	0,254	0,064	64,948	65,302	64,585	65,545	0,391	-0,540	0,420	0,480	65,142	65,108	0,249	0,276	0,000	0,000
Zy(l)-Tr(l)	28,648	0,243	0,061	28,479	28,817	28,379	29,296	0,850	-0,269	0,648	0,459	28,697	28,600	0,302	0,174	0,000	0,000
Zy(r)-Tr(r)	30,602	0,422	0,106	30,309	30,895	29,643	31,259	1,380	-0,959	0,657	0,808	30,557	30,647	0,397	0,470	0,002	0,010
Ch(r)-Tr(r)	82,489	0,404	0,101	82,209	82,770	81,633	83,077	0,490	-0,856	0,588	0,722	82,395	82,584	0,433	0,377	0,000	0,018
Ch(l)-Tr(l)	81,869	0,284	0,071	81,672	82,067	81,464	82,366	0,347	-0,405	0,497	0,451	81,790	81,949	0,325	0,231	0,000	0,001
Ch(r)-Gn(r)	54,065	0,350	0,087	53,822	54,307	53,010	54,498	0,647	-1,055	0,433	0,744	54,084	54,045	0,145	0,490	0,002	0,001
Ch(l)-Gn(l)	52,015	0,153	0,038	51,909	52,121	51,644	52,267	0,294	-0,370	0,252	0,311	52,036	51,994	0,192	0,109	0,000	0,000

Table 10. Comparison of measurements obtained at different rolling degrees to the right and to the left: mean, standard deviation (dev.st), standard error (err.st); lower 95% confidence interval (CI95% Low), high 95% confidence interval (CI95% high), minimum value (min), maximum value (max), variation coefficient (CV), difference between minimum and mean value (d_min), difference between minimum and mean value (d_min), maximum error (error_m).

Pitch

The same assessments were made for the pitching movement (Table 11).

FISSOvsBECC.	media	dev.st	err.st	min	max	CV	CI95%Low	CI95%High	d_min	d_max	errore_m	media_fisso	media_becc	sd_fisso	sd_becc	p-value (A>B)	p-value (B>A)
Chel(r)-Chel(l)	54,837	0,224	0,054	54,278	55,288	0,409	53,144	55,412	-0,559	0,451	0,505	54,849	54,823	0,284	0,148	0,000	0,000
N-Pronasale	42,755	0,288	0,070	42,182	43,285	0,674	40,309	44,055	-0,573	0,530	0,551	42,646	42,876	0,329	0,185	0,000	0,002
Sn-Pg	56,739	0,192	0,047	56,484	57,197	0,339	55,543	57,425	-0,255	0,458	0,357	56,792	56,679	0,231	0,125	0,000	0,000
N-Pg	105,162	0,238	0,058	104,816	105,684	0,226	104,187	105,444	-0,346	0,522	0,434	105,246	105,068	0,287	0,127	0,000	0,000
Glab-Ch(r)	67,693	0,242	0,059	67,035	68,042	0,358	66,041	68,029	-0,658	0,349	0,504	67,675	67,714	0,188	0,305	0,000	0,000
Glab-Ch(l)	68,074	0,220	0,053	67,764	68,644	0,324	66,866	68,663	-0,310	0,570	0,440	68,132	68,009	0,264	0,149	0,000	0,000
Glab-Ft(r)	65,677	0,140	0,034	65,441	65,998	0,212	64,851	66,031	-0,236	0,321	0,279	65,664	65,691	0,108	0,176	0,000	0,000
Glab-Ft(l)	65,346	0,269	0,065	64,892	65,691	0,412	63,750	66,035	-0,453	0,345	0,399	65,518	65,152	0,167	0,230	0,005	0,000
Zy(l)-Tr(l)	28,761	0,559	0,136	27,539	29,507	1,945	22,139	32,940	-1,222	0,746	0,984	29,144	28,330	0,215	0,512	0,510	0,000
Zy(r)-Tr(r)	30,814	0,382	0,093	30,389	31,696	1,238	26,951	33,827	-0,425	0,882	0,654	30,961	30,647	0,425	0,258	0,030	0,000
Ch(r)-Tr(r)	82,493	0,241	0,059	82,202	82,973	0,292	81,390	83,014	-0,291	0,480	0,386	82,572	82,403	0,272	0,176	0,000	0,000
Ch(l)-Tr(l)	82,026	0,502	0,122	80,902	82,839	0,613	79,201	82,602	-1,124	0,813	0,969	82,364	81,645	0,335	0,368	0,166	0,000
Ch(r)-Gn(r)	54,032	0,140	0,034	53,803	54,286	0,259	53,084	54,522	-0,229	0,254	0,241	53,982	54,088	0,138	0,128	0,000	0,000
Ch(l)-Gn(l)	51,953	0,166	0,040	51,673	52,284	0,319	50,788	52,558	-0,280	0,331	0,305	51,886	52,029	0,180	0,115	0,000	0,000

Table 11. Comparison of the measurements obtained by shots at 0 degrees with those obtained at different degrees of pitch upward: mean, standard deviation (dev.st), standard error (err.st); lower 95% confidence interval (CI95% Low),

high 95% confidence interval (CI95% high), minimum value (min), maximum value (max), variation coefficient (CV), difference between minimum and mean value (d_min), difference between minimum and mean value (d_min), maximum error (error_m).

The two sets of measurements were significantly equivalent ($p < 0.05$) with the exception of two distances: *Zygion*(l)-*Tragion*(l) ($p = 0.510$) and *Cheek*(l)-*Tragion*(l) (p = 0.166). The maximum difference between the averages was 0.814 mm calculated for *Zygion*(l)-*Tragion*(l).

Subsequently, low and high pitch rates were compared. The measurements were equivalent ($p <0.05$) with a maximum difference between the mean of the 0.238 mm *Cheek*(l)-*Tragion*(l) measurement (Table 12).

BECCHEGGIO	media	dev.st	err.st	CI95%Low	CI95%High	min	max	CV	d_min	d_max	errore_m	media_bassa	media_alta	sd_bassa	sd_alta	p-value (A>B)	p-value (B>A)
Chel(r)-Chel(l)	54,799	0,129	0,032	54,709	54,888	54,599	55,080	0,236	-0,200	0,281	0,241	54,768	54,829	0,114	0,143	0,000	0,000
N-Pronasale	42,869	0,182	0,045	42,743	42,996	42,458	43,147	0,424	-0,411	0,277	0,344	42,835	42,904	0,204	0,162	0,000	0,000
Sn-Pg	56,676	0,146	0,037	56,574	56,778	56,484	56,929	0,258	-0,192	0,253	0,222	56,731	56,621	0,154	0,124	0,000	0,000
N-Pg	105,034	0,151	0,038	104,929	105,139	104,680	105,256	0,144	-0,353	0,222	0,288	105,050	105,017	0,178	0,130	0,000	0,000
Glab-Ch(r)	67,670	0,254	0,063	67,494	67,846	67,035	67,967	0,375	-0,635	0,297	0,466	67,607	67,733	0,280	0,225	0,000	0,000
Glab-Ch(l)	68,050	0,170	0,042	67,932	68,167	67,764	68,341	0,250	-0,285	0,291	0,288	68,024	68,076	0,159	0,187	0,000	0,000
Glab-Ft(r)	65,638	0,203	0,051	65,498	65,779	65,111	65,998	0,309	-0,528	0,360	0,444	65,642	65,634	0,183	0,233	0,000	0,000
Glab-Ft(l)	65,199	0,193	0,048	65,065	65,333	64,892	65,536	0,296	-0,307	0,337	0,322	65,189	65,209	0,176	0,221	0,000	0,000
Zy(l)-Tr(l)	28,434	0,477	0,119	28,103	28,765	27,539	29,124	1,676	-0,895	0,690	0,792	28,452	28,415	0,614	0,330	0,011	0,006
Zy(r)-Tr(r)	30,496	0,371	0,093	30,238	30,754	29,855	31,108	1,217	-0,641	0,612	0,627	30,510	30,482	0,352	0,413	0,002	0,001
Ch(r)-Tr(r)	82,248	0,382	0,096	81,983	82,514	81,235	82,687	0,465	-1,013	0,439	0,726	82,318	82,178	0,259	0,485	0,009	0,000
Ch(l)-Tr(l)	81,727	0,397	0,099	81,451	82,002	80,775	82,149	0,486	-0,952	0,422	0,687	81,608	81,846	0,509	0,216	0,000	0,025
Ch(r)-Gn(r)	54,103	0,147	0,037	54,001	54,204	53,838	54,354	0,271	-0,264	0,251	0,258	54,059	54,147	0,143	0,145	0,000	0,000
Ch(l)-Gn(l)	51,987	0,129	0,032	51,898	52,076	51,754	52,284	0,247	-0,233	0,296	0,265	52,013	51,962	0,132	0,129	0,000	0,000

Table 12. Comparison of measurements obtained at low and high pitch rates: mean, standard deviation (dev.st), standard error (err.st); lower 95% confidence interval (CI95% Low), 95% confidence interval (CI95% high), minimum value (min), maximum value (max), variation coefficient (CV), difference between the minimum and mean value (d_min), the difference between the minimum and mean value (d_min), the maximum error (error_m)

Comparisons were also made of the inclination of the head downward and upward, during the pitch movement. The data (Table 13) showed a substantial equivalence (p <0.05) between the two sets of measurements. The maximum difference between the averages is 0.310 mm in the *Cheek*(r)-*Tragion*(r) measurement.

BECCHEGGIO +/-	media	dev.st	err.st	CI95%Low	CI95%High	min	max	CV	d_min	d_max	errore_m	media +	media -	sd -	sd +	p-value (A>B)	p-value (B>A)
Chel(r)-Chel(l)	54,799	0,129	0,032	54,709	54,888	54,599	55,080	0,236	-0,200	0,281	0,241	54,823	54,774	0,148	0,112	0,000	0,000
N-Pronasale	42,869	0,182	0,045	42,743	42,996	42,458	43,147	0,424	-0,411	0,277	0,344	42,876	42,863	0,185	0,191	0,000	0,000
Sn-Pg	56,676	0,146	0,037	56,574	56,778	56,484	56,929	0,258	-0,192	0,253	0,222	56,679	56,673	0,125	0,174	0,000	0,000
N-Pg	105,034	0,151	0,038	104,929	105,139	104,680	105,256	0,144	-0,353	0,222	0,288	105,068	104,999	0,127	0,174	0,000	0,000
Glab-Ch(r)	67,670	0,254	0,063	67,494	67,846	67,035	67,967	0,375	-0,635	0,297	0,466	67,714	67,626	0,305	0,202	0,000	0,000
Glab-Ch(l)	68,050	0,170	0,042	67,932	68,167	67,764	68,341	0,250	-0,285	0,291	0,288	68,009	68,090	0,149	0,190	0,000	0,000
Glab-Ft(r)	65,638	0,203	0,051	65,498	65,779	65,111	65,998	0,309	-0,528	0,360	0,444	65,691	65,585	0,176	0,225	0,000	0,000
Glab-Ft(l)	65,199	0,193	0,048	65,065	65,333	64,892	65,536	0,296	-0,307	0,337	0,322	65,152	65,246	0,230	0,149	0,000	0,000
Zy(l)-Tr(l)	28,434	0,477	0,119	28,103	28,765	27,539	29,124	1,676	-0,895	0,690	0,792	28,330	28,538	0,512	0,447	0,001	0,041
Zy(r)-Tr(r)	30,496	0,371	0,093	30,238	30,754	29,855	31,108	1,217	-0,641	0,612	0,627	30,647	30,345	0,258	0,420	0,031	0,000
Ch(r)-Tr(r)	82,248	0,382	0,096	81,983	82,514	81,235	82,687	0,465	-1,013	0,439	0,726	82,403	82,093	0,176	0,477	0,037	0,000
Ch(l)-Tr(l)	81,727	0,397	0,099	81,451	82,002	80,775	82,149	0,486	-0,952	0,422	0,687	81,645	81,808	0,368	0,433	0,000	0,013
Ch(r)-Gn(r)	54,103	0,147	0,037	54,001	54,204	53,838	54,354	0,271	-0,264	0,251	0,258	54,088	54,118	0,128	0,171	0,000	0,000
Ch(l)-Gn(l)	51,987	0,129	0,032	51,898	52,076	51,754	52,284	0,247	-0,233	0,296	0,265	52,029	51,946	0,115	0,135	0,000	0,000

Table 13. Comparison of measurements obtained at different pitches up and down: mean, standard deviation (dev.st), standard error (err.st); lower 95% confidence interval (CI95% Low), high 95% confidence interval (CI95% high), minimum value (min), maximum value (max), variation coefficient (CV), difference between the minimum and mean value (d_min), the difference between the minimum and mean value (d_min), the maximum error (error_m).

The data shown show a substantial equivalence of the measurements carried out with different angular degrees on the three planes of the space.

Only in two isolated values, in the series of measurements obtained with different degrees of pitch up and compared with those obtained with the dummy at 0 degrees, a non-equivalence of the measurements was found; specifically, they are *Zygion*(l)-*Tragion*(l) and *Cheek*(l)-*Tragion*(l) measurements upwards.

7.5 Part II (in vivo)

From the analysis of the data obtained in the reference position (5 shots in NHP per patient), it was possible to define a maximum in vivo reproducibility error of the system, useful in subsequent surveys for the definition of the equivalence limit (Fig. 17).

As can be seen in the graph, the maximum recorded reproducibility error is 1.214 mm (recorded in *Zygio*n(r)-*Tragion*(r) region and indicated by the arrow (Fig. 17); this was the value used in the statistical analysis as the maximum difference accepted between the series of measurements to support the statistical equivalence of the obtained values.

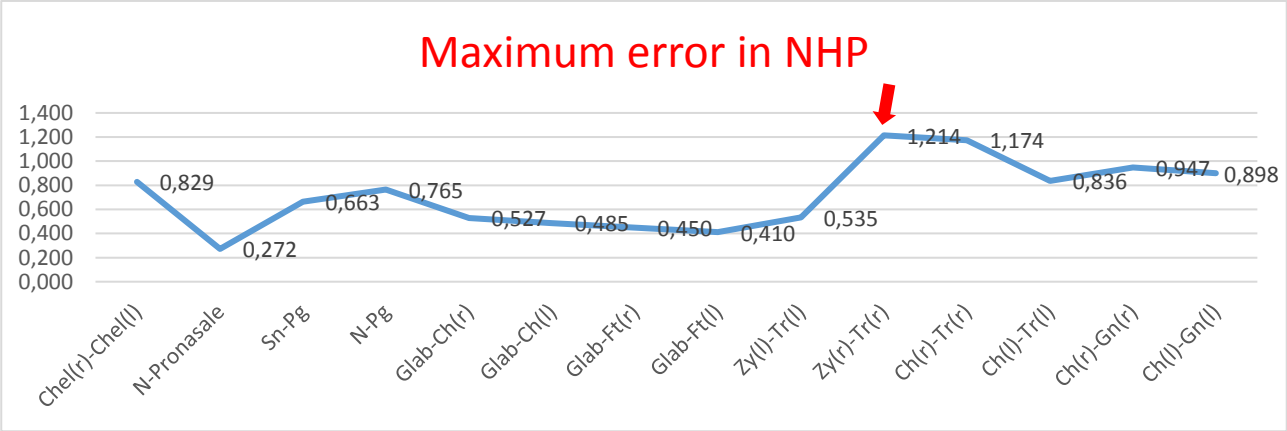

Figure 17. Maximum error in NHP.

For each student, a comparison was made between the measurements obtained with the head angled in the three planes of the space and the average of the values recorded in the NHP in order to statistically analyse the data and to detect any statistical difference (p <0.05).

Measurements	***Equivalence* (yaw, roll, pitch)**	
	4°	*8°*
Chel(r)-Chel(l)	**y**	**y**
N-Prn	**y**	**y**
Sn-Pg	**y**	**n**
N-Pg	**y**	**n**
Glab-Ch(r)	**y**	**y**
Glab-Ch(l)	**y**	**y**
Glab-Ft(r)	**y**	**y**
Glab-Ft(l)	**y**	**y**
Zy(r)-Tr(r)	**n**	**n**
Zy(l)-Tr(l)	**n**	**n**
Ch(r)-Tr(r)	**n**	**n**
Ch(l)-Tr(l)	**n**	**n**
Ch(r)-Gn(r)	**y**	**n**
Ch(l)-Gn(l)	**y**	**n**

Table 14. Results of the equivalence tests performed between the average of the values in the reference position and the angles of 4 and 8 degrees in the three planes of space (**y**=equivalent, **n**=non-equivalent)

Summary statistics for all students measurements were calculated for both the angulations (Table 14); statistically significant difference were reported for the following measurements: *Zygion*(r)-*Tragion*(r), *Zygion*(l)-*Tragion*(l), *Cheek*(r)-*Tragion*(r), *Cheek*(l)-*Tragion*(l) for angles of 4 degrees of pitch, roll and yaw in both directions (right/left, high/low). In larger angles (8 degrees) statistically significant differences were reported also in these measurements: *Subnasale-Pogonion*, *Nasion-Pogonion*, *Cheek*(r)-*Gonion*(r), *Cheek*(l)-*Gonion*(l).

In Figure 18 was performed the graphic overlap between the shots in the NHP and the 8-degrees rotation of the head to the right. It is possible to appreciate, with the help of colorimetric map, that the major differences (red areas) are located in the most lateral regions (*Tragion, Gonion*) and at *Cheek* and *Pogonion* points.

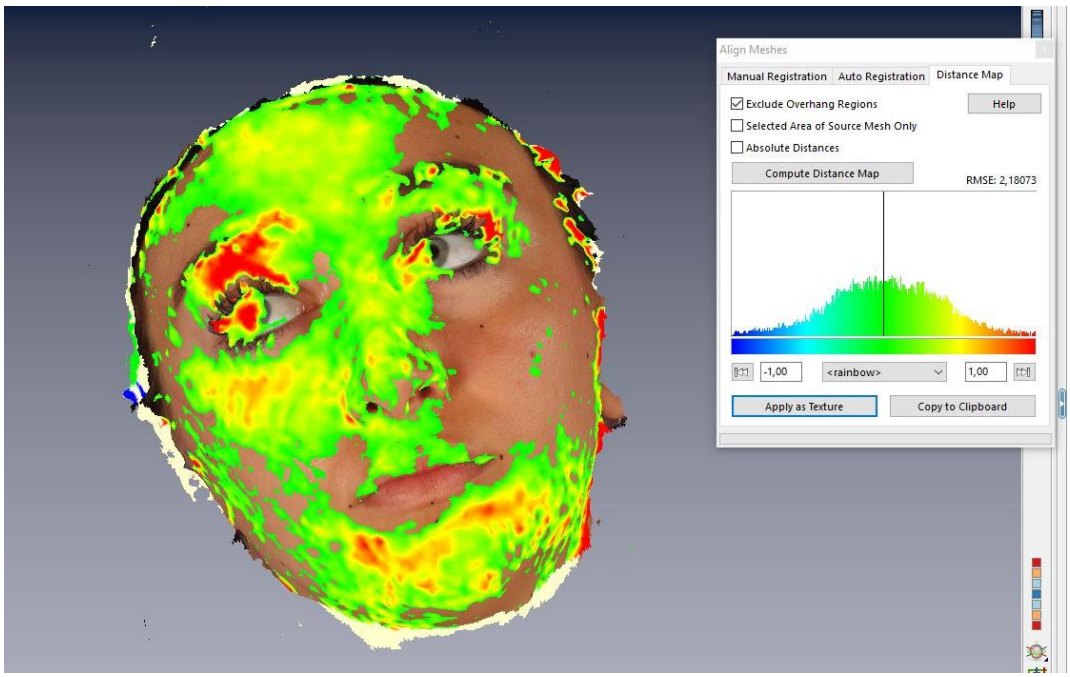

Figure 18. Overlap of two positions and colorimetric map.

8. DISCUSSION AND CONCLUSIONS

Because of the paradigm shift from hard to soft tissue and considering the results of the most recent literature, the role of stereofotogrammetry in orthodontic diagnosis and maxillofacial pre- and post-surgical evaluation is becoming increasingly important. Facial scanning systems are continuously being developed, and the major concern about these new systems is reproducibility and reliability of the measurements obtained from the facial scans. Our goal was to analyse a new 6-camera stereofotogrammetry system and to evaluate the accuracy and the reliability of the measurements obtained. In particular, the analysis focused on searching for errors, whether they are specific to the system or related to the operator.

A previous study [135] have demonstrated that landmarks have not the same reproducibility dividing them into highly, moderately and poorly reproducible landmarks. Examples such as Zygion, Gonion, and Tragion have been shown to have poor reproducibility. In this study, the highest maximum error was recorded in the measurements involving the Tragion on both the dummy and the students. Since in this study we cross-registered the complete facial data (including ears) of the various measurements, which are the most variable. We can assume that removal of these parts, reducing the measurements onto the facial oval, would improve the precision. In fact, if we exclude measurements made in the lateral regions, the maximum error recorded drops considerably (0.535 *vs* 0.89 mm *in vitro*/0.947 *vs* 1.214 mm *in vivo*). This will be the subject of future investigations.

In the present study, all facial scan were taken in NHP; other standardization criterions for the scanning procedure was the selection of participants from the subjects within the healthy percentage according to body mass index and to mark the anthropometric points on the subject's face before the shots in order to reproduce them more easily on the texture. This may have led the examiners to encounter more standardized soft tissue identifications.

Intra-operator maximum error was very low (0.334 mm), acquisition error and inter-operator error were very similar (0.496mm/0.532 mm); reproducibility maximum error was the higher, as aspected

(0.89 mm). These results agree with data from studies conducted with other stereophotogrammetry systems[136,137]. Ayoub *et al* [138] identified operator error to be accurate within 0.2 mm and the average discrepancy of point location for three operator involved was 0.79 mm.

Apart from the system error and registration error, several other factors might influence the accuracy of the registration. One of this is the ability to capture the face in the same facial expression every time. Because a 3D photograph is a static picture, captures only in one moment, facial expression sometimes can be of great influence to reproducibility. The ability to reproduce the face at rest is a highly important factor for preoperative and postoperative evaluation of treatment changes. If the variation within the face at rest is large, the evaluation of surgery based on preoperative and postoperative 3D photographs is inaccurate. Jonhston et al[139] found a reproducibility of 0.74 mm for the face at rest.

Also positioning of the individual might also influence the accuracy of registration. To minimize this influence, the head is normally positioned in NHP. In a recent study, Zhu *et al*[140] determined the intra-rater and interrater reliability of reorientating three-dimensional (3D) facial images into the estimated natural head position. Three-dimensional facial images of 15 pre-surgical class III orthognathic patients were obtained and automatically re-orientated into natural head position (RNHP) using a 3d stereophotogrammetry system and in-hose software. Six clinicians were asked to estimate the NHP of these patients (ENHP); they re-estimated five randomly selected 3D images after 2-week interval. The differences in yaw, roll, pitch and chin position between RNHP and ENHP were measured. For intra-rater reliability, the intra-class correlation coefficient (ICC) values ranges from 0.55 to 0.77, representing moderate reliability for roll, yaw, pitch, and chin position, while for inter-rater reliability, the ICC values ranges from 0.38 to 0.58, indicating poor to moderate reliability. The median difference between ENHP and RNHP was small for roll and yaw, but larger for pitch. There was a tendency for the clinicians to estimate NHP with the chin tipped more posteriorly (6.3±5.2 mm) compared to RNHP, reducing the severity of the skeletal deformity in anterior-posterior direction.

Another interesting study was proposed by Hughes *et al*[141] to determine whether an observer's perception of the correct anatomical alignment of the head changes with time, and whether different observers agree on the correct anatomical alignment. To determine whether the perception of the correct anatomical alignment changes with time (intra-observer comparison), a group of 30 observers were asked to orient, into anatomical alignment, the three-dimensional (3D) head photograph of a normal man, on two separate occasions. To determine whether different observers agree on the correct anatomical alignment (inter-observer comparison), the observed orientations were compared. The results of intra-observer comparisons showed substantial variability between the first and second anatomical alignments. Bland-Altman coefficients of repeatability for pitch, yaw, and roll, were 6.9°, 4.4°, and 2.4°, respectively. The results of inter-observer comparisons showed that the agreement for roll was good (sample variance 0.4, standard deviation (SD) 0.7°), the agreement for yaw was moderate (sample variance 2.0, SD 1.4°), and the agreement for pitch was poor (sample variance 15.5, SD 3.9°). In conclusion, the perception of correct anatomical alignment changes considerably with time. Different observers disagree on the correct anatomical alignment. Agreement among multiple observers was bad for pitch, moderate for yaw, and good for roll.

Maal *et al*[142] have proposed a prospective study to determine variations in the face at rest; 100 3D photographs of the same individual were acquired at different times. Initially, 50 3D photographs were obtained; 25 using a wax bite to ensure similar occlusion between subsequent photographs and 25 without wax bite. This procedure was repeated 6 weeks later. Variation of the face at rest was computed. The influence of time and wax bite was investigated. Different anatomical regions were investigated separately. A mean variation of 0.25 mm (0.21-0.27 mm) was found (standard deviation 0.157 mm). No large differences were found between different time points or use of wax bite. Regarding separate anatomical regions, there were small variations in the nose and forehead regions; the largest variations were found in the mouth and eyes. This study showed small overall variation within the face at rest. In conclusion, different 3D photographs can be reproduced accurately and used in a clinical setting for treatment follow-up and evaluation.

To the best our knowledge, no studies have been performed to investigate the accuracy of our stereophotogrammetric system in a clinical setting and there are no studies on soft tissue variations induced by head rotations in the three planes of space. NHP may be difficult to reach in some patients, especially in children, in patients with neuromuscular disorders, vertebral column deformity and alterations in eye muscles balancing. We chose to use rotation entities of 4 and 8 degrees because included in that patient's variability in NHP.

Within the different anatomical units, the most accurate values were found in the region of forehead and the nose. In vivo the most variations were found in lateral region (*Zygion, Tragion, Gonion*); in acquisitions with 8 degrees of rotations we found a statistical difference also for measurements involving the Pogonion; it might have been caused because the data point was located at the edge of the system field of view and prone to light distortion. The same reason could explain the inconsistencies we found in soft-tissue measurements that included tragion, which also lies on the edge of the field of view.

Also in our study the mouth is a region of large mobility, but the use of a wax bite does not improve this aspect[141]. A possible explanation is that, when movements occurs, these movements are within the soft tissue (especially cheek and mouth region) due to muscular activity, whereas the wax bite only fixates the mandibular bon on the maxilla. The issue of occlusion in the NHP remains controversial: in maximal intercuspidation the posture of the lips and the morphology are modified and the face is not at rest; also with first tooth contact and ‘in centric relation’ does not always reproduce the face at rest.

In conclusion, we can state that the Face Shape 3D Maxi Line has sufficient accuracy for orthodontic and surgical use, especially in the median areas of the face. Despite the presence of areas of non-equivalence the differences are however clinically acceptable.

Taking into account the magnitude of the intra- and inter-operator error, which represent a significant proportion of the total error, one might think that acting on them and on the learning curve can reduce the system error.

It also seems that such precision is not altered by the rotation of the head on three planes of space (both *in vitro* and *in vivo*), making the acquisition process even simpler and less constrained to a predetermined position, which is not always easy to obtain with all patients. This improves the comparison of acquisitions obtained in different times and conditions, facilitating the clinician during a long-term treatment.

Lateral regions, along with interoperability variability, are sources of greater acquisition and reproducibility errors, especially in measurements involving the Tragion area. Further studies are needed to confirm the results obtained *in vivo* by increasing the sample size and by examining subjects belonging to different age ranges (thickness and soft tissue characteristics).

REFERENCES

[1] Sforza C, de Menezes M, Ferrario VG. *Soft-and hard-tissue facial anthropometry in three dimensions: what's new.* J Anthropol Sciences 2013; 91:159-84.

[2] Borah GL, Rankin MK. *Appearance is a function of the face.* Plast Reconstr Surg 2010; 125:873-8.

[3] Smeets D, Claes P, VAndermeulen D, Clement JG. *Objective 3D face recognition: evolution approaches and challenges.* Forensic Sci Int 2010; 201:125:32.

[4] Grill-Spector K, Knouf N, Kanwisher N. *The fusiform face area subseries face perception, not generic within-category identification.* Nat Neurosci 2004; 7:555-62.

[5] Fourie Z, Damastra J, Gerrits PO, Ren Y. *Evaluation and anthropometric accuracy and reliability using different three-dimensional scanning systems.* Forensic Sci Int 2011; 207:127-34.

[6] Farkas LG, Bryson W, Klots J. *Is photogrammetry of the face reliable?* Plast Reconstr Surg 1980; 66:346-55.

[7] Lubbers H-T, Medinger L, Kruse A, Gratz KW, Matthews F. *Precision and accuracy of the 3dMD photogrammetric system in craniomaxillofacial application.* J Craniofac Surg 2010; 21:763-67.

[8] Kau CH, Richmond S, Incrapera A, English J, Xia JJ. *Three-diemnsional surface acquisition systems for the study of facial morphology and their application to maxillofacial surgery.* Int J Med Robot 2007; 3:97-110.

[9] http://www.treccani.it/enciclopedia/antropometria

[10] Carolus Linnaeus. *Systema Naturae.* Theodorum Haak, Rotterdam,1735.

[11] Quetelet. *Average Man.* Edinburgh Medical Journal, 1842.

[12] Da Costa Martins D. *Height, weight and chest circumference of children of different ethnic groups in Lourenço Marques, Moçambique, in 1965 with a note on the secular trend.* Hum Biol. 1971; 43:253-64.

[13] Karn MN, Penrose LS. *Birth weight and gestation time in relation to maternal age, parity and infant survival.* Ann Eugen. 1952; 16:147-64.

[14] Thurstone LL. *Factorial analysis of body measurements.* Am J Phys Anthropol 1947; 5:15-28.

[15] Tanner JM. *Growth and maturation during adolescence.* Nutr Rev 1981; 39:43-55.

[16] Abernathy JR, Greenberg BG, Grizzle JE, Donnelly JF. *Birth weight, gestation, and crown-heel length as response variables in multivariate analysis.* Am J Public Health Nations Health 1966; 56:1281-6.

[17] Hrdlicka A. *Anthropometry.* American Journal of Physical Anthropology 1919; 2:401-28.

[18] Barrier P, Dedouit F, Braga J, Joffre F, Rouge D, Rousseau H, Telmon N. *Age at death estimation using multislice computed tomography reconstructions of the posterior pelvis.* J Forensic Sci 2009; 54:773–8.

[19] van den Heever D, Scheffer C, Erasmus P, Dillon E. *Classification of gender and race in the distal femur using self organising maps*. Knee 2012; 19:488-92.

[20] Barnes CL, Iwaki H, Minoda Y, Green JM 2nd, Obert RM. *Analysis of sex and race and the size and shape of the distal femur using virtual surgery and archived computed tomography images.* J Surg Orthop Adv 2010; 19:200-8.

[21] Vaidya SV, Ranawat CS, Aroojis A, Laud NS. *Anthropometric measurements to design total knee prostheses for the Indian population.* J Arthroplasty 2000;15:79-85.

[22] Milić M, Grgantov Z, Chamari K, Ardigò LP, Bianco A, Padulo J. *Anthropometric and physical characteristics allow differentiation of young female volleyball players according to playing position and level of expertise.* Biol Sport 2017; 34:19-26.

[23] Sandler V, Reisetter AC, Bain JR, Muehlbauer MJ, Nodzenski M, Stevens RD, Ilkayeva O, Lowe LP, Metzger BE, Newgard CB, Scholtens DM, Lowe WL Jr. *Associations of maternal BMI and insulin resistance with the maternal metabolome and newborn outcomes.* Diabetologia 2017; 60:518-30.

[24] Shin YH, Choi SJ, Kim KW, Yu J, Ahn KM, Kim HY, Seo JH, Kwon JW, Kim BJ, Kim HB, Shim JY, Kim WK, Song DJ, Lee SY, Lee SY, Jang GC, Kwon JY, Lee KJ, Park HJ, Lee PR, Won HS, Hong SJ. *Association between maternal characteristics and neonatal birth weight in a Korean population living in the Seoul metropolitan area, Korea: a birth cohort study (COCOA).* J Korean Med Sci 2013; 28:580-5.

[25] Jackson J, Hamar B, Lazar E, Lim K, Rodriguez D, Stock K, Wolfberg AJ, Dunk R. *Nuchal translucency measurement plus non-invasive prenatal testing to screen for aneuploidy in a community-based average-risk population.* Ultrasound Obstet Gynecol 2014; 44:491.

[26] Galjaard S, Pasman SA, Ameye L, Timmerman D, Devlieger R. *Intima-media thickness measurements in the fetus and mother during pregnancy: a feasibility study.* Ultrasound Med Biol 2014; 40:1949-57.

[27] Malone SK, Zemel BS. *Measurement and Interpretation of Body Mass Index During Childhood and Adolescence.* J Sch Nurs 2015; 31:261-71.

[28] Melunovic M, Hadzagic-Catibusic F, Bilalovic V, Rahmanovic S, Dizdar S. *Anthropometric Parameters of Nutritional Status in Children with Cerebral Palsy.* Mater Sociomed 2017; 29:68-72.

[29] Kim YK, Lee NK, Moon SW, Jang MJ, Kim HS, Yun PY. *Evaluation of soft tissue changes around the lips after bracket debonding using three-dimensional stereophotogrammetry.* Angle Orthod 2015; 85:833-40.

[30] Taylor HO, Morrison CS, Linden O, Phillips B, Chang J, Byrne ME, Sullivan SR, Forrest CR. *Quantitative facial asymmetry: using three-dimensional photogrammetry to measure baseline facial surface symmetry.* J Craniofac Surg 2014; 25:124-8.

[31] Brevi B, Di Blasio A, Di Blasio C, Piazza F, D'Ascanio L, Sesenna E. *Which cephalometric analysis for maxillo-mandibular surgery in patients with obstructive sleep apnoea syndrome?* Acta Otorhinolaryngol Ital. 2015; 35:332-7.

[32] Velemínská J, Katina S, Smahel Z, Sedlácková M. *Analysis of facial skeleton shape in patients with complete unilateral cleft lip and palate: geometric morphometry.* Acta Chir Plast 2006; 48:26-32.

[33] Holdaway RA. *A soft tissue cephalometric analysis and its use in orthodontic treatment planning. Part I.* Am J Orthod 1983; 84:1-28.

[34] Worms FW, Spiedel TM, Bevis RR, Waite DE. *Posttreatment stability and esthetics of orthognathic surgery.* Angle Orthod 1980; 50:251-73.

[35]Burstone CJ. *Lip posture and its significance in treatment planning.* Am J Orthod 1967; 53:262-84.

[36] Burstone CJ. *The integumental profile.* Am J Orthod 1958; 44:1-25.

[37] Michiels LYF, Tourne LPM. *Nasion true vertical: a proposed method for testing the clinical validity of cephalometric measurements applied to a new cephalometric reference line.* Int JAdult Orthod Orthog Surg 1990; 5:43-52.

[38] Park YC, Burstone CJ. *Soft tissue profile: fallacies of hard tissue standards in treatment planning.* Am J Orthod Dentofacial Orthop 1986; 90:52-62.

[39] Holdaway RA. *A soft tissue cephalometric analysis and its use in orthodontic treatment planning. Part II.* Am J Orthod 1984; 85:279-93.

[40] Legan HL, Burstone CJ. *Soft tissue cephalometric analysis for orthognathic surgery.* J Oral Surg 1980; 38:744-51.

[41] Arnett GW, Jelic JS, Kim J, Cummings DR, Beress A, Worley CM Jr, Chung B, Bergman R. *Soft tissue cephalometric analysis: diagnosis and treatment planning of dentofacial deformity.* Am J Orthod Dentofacial Orthop 1999; 116:239-53.

[42] Arnett GW, Bergman RT. *Facial keys to orthodontic diagnosis and treatment planning. Part I.* Am J Orthod Dentofacial Orthop 1993; 103:299-312.

[43] Arnett GW, Bergman RT. *Facial keys to orthodontic diagnosis and treatment planning. Part II.* Am J Orthod Dentofacial Orthop 1993; 103:395-411.

[44] Baysal A, sahan AO, Ozturk MA, Uysal T. *Reproducibility and reliability of three-dimensional soft tissue landmark identification using three-dimensional stereophotogrammetry.* Angle Orthod 2016; 86:1004-9.

[45] Sarver DM, Ackerman JL. *Orthodontics about face: the re-emergence of the aesthetic paradigm.* Am J Orthod Dentofacial Orthod 2000; 117:575-6.

[46] Farkas LG, Posnick JC, Hreczko TM. *Anthropometric growth study of the head.* Cleft Palate Craniofac J 1992; 29:303-8.

[47] Elder R, Wertheim D, Greenhill D. *Comparison of radiographic and photographic measurement of mandibular asymmetry.* Am J Orthod Dentofacial Orthop 2003; 123:167-74.

[48] Cutting CB, McCarthy JG, Karron DB. *Three-dimensional input of body surface data using a laser light scanner.* Ann Plast Surg 1988; 21:38-45.

[49] Broadbent BS. *A new X-ray technique and its application to orthodontia.* Angle Orthod 1931; 1:45-66.

[50] Singh IJ, Savara BS. *Norms of size and annual increments of seven anatomical measures of maxillae in girls from three to sixteen years of age.* Angle Orthod 1966; 36:312-24.

[51] Burke PH, Beard FH. *Stereophotogrammetry of the face. A preliminary investigation into the accuracy of a simplified system evolved for contour mapping by photography.* Am J Orthod 1967; 53:769-82.

[52] Udupa J, Herman G. *3D Imaging in Medicine.* Boca Raton: CRC Press, 1991.

[53] Hajeer MY, Millet DT, Ayoub AF, Siebert JP. *Application of 3D imaging in orthodontics: Part I.* J Orthod 2004; 31:62-70.

[54] Baumrind S. *Integrated three-dimensional craniofacial mapping: background, principles, and perspectives.* Semin Orthod 2001; 7:223-32.

[55] Sforza C, de Menezes M, Ferrario VG. *Soft-and hard-tissue facial anthropometry in three dimensions: what's new.* J Anthropol Sciences 2013; 91:159-84.

[56] Swennen GR, Mollemans W, Schutyser F. *Three-dimensional treatment planning of orthognathic surgery in the era of virtual imaging.* J Oral Maxillofac Surg 2009; 67:2080-92.

[57] https://it.wikipedia.org/wiki/Risonanza_magnetica_nucleare

[58] See MS, Foxton MR, Miedzianowski-Sinclar NA, Robert C, Nduka C. *Stereophotogrammetric measurements of the nasolabial fold in repose: a study of age and posture-related changes.* Eur J Plast Surg 2007; 29:387-93.

[59]Swennen GRJ, Schutyser F, Lemaitre A, Malevez C, De Mey A. *Accuracy and reliability of 3-D CT versus 3-D stereo photogrammetry based facial soft tissue analysis*. Int J Oral Maxillofac Surg 2005; 34:73.

[60]Galantucci LM, Ferrandes R, Percoco G. *Digital photogrammetry for facial recognition.* J Comput Inf Sci Eng 2006; 4:390-6.

[61]Galantucci LM, Percoco G, Dal MU. *Coded targets and hybrid grids for photogrammetric 3D digitisation of human faces.* Virtual Phys Prototyp 2008; 3:167-76.

[62] Ettorre G, Weber M, Schaaf H, Lowry JC, Mommaerts MY, Howaldt HP. *Standards for digital photography in cranio-maxillo-facial surgery - Part I: Basic views and guidelines.* J Craniomaxillofac Surg 2006; 34:65-73.

[63] Schaaf H, Streckbein P, Ettorre G, Lowry JC, Mommaerts MY, Howaldt HP. *Standards for digital photography in cranio-maxillo-facial surgery--part II: additional picture sets and avoiding common mistakes.* J Craniomaxillofac Surg 2006; 34: 444-55.

[64]Mollemans W, Schutyser F, Nadjmi N, Maes F, Suetens P. *Predicting soft tissue deformations for a maxillofacial surgery planning system: from compu- tational strategies to a complete clinical validation.* Med Image Anal 2007; 11: 282-301.

[65]Olszewski R, Villamil MB, Trevi- san DG, Nedel LP, Freitas CM, Rey- chler H, Macq B. *Towards an integrated system for planning and assisting maxillofacial orthognathic surgery*. Comput Methods Programs Biomed 2008; 91: 13-21.

[66]Kaplan HM. *A pioneer in 3-D technology for medical imaging: 3dMD.* Technol Commercial Alliance 2003: 70-82.

[67] Maal TJ, Plooij JM, Rangel FA, Mollemans W, Schutyser FA, Berge SJ. *The accuracy of matching three- dimensional photographs with skin surfaces derived from cone-beam computed tomography.* Int J Oral Maxillofac Surg 2008: 37: 641-6.

[68] Hell B, Walter FA, Schreiber S, Blase H, Bielke G, Meindl S, Stein G. *Three-dimensional ultrasonography in maxillofacial surgery. A new diagnostic tool.* Int J Oral Maxillofac Surg 1993: 22:173-7.

[69] Kau CH, Cronin AJ, Richmond S. *A three-dimensional evaluation of postoperative swelling following orthognathic surgery at 6 months.* Plast Reconstr Surg 2007; 119:2192-9.

[70] Kau CH, Zhurov A, Scheer R, Bouwman S, Richmond S. *The feasibility of measuring three-dimensional facial morphology in children.* Orthod Craniofac Res 2004; 7:198-204.

[71] Joanneke M. Plooij, Thomas J. J. Maal, Piet Haers, Wilfred A. Borstlap, Anne Marie Kuijpers-Jagtman, Stefaan J. Berge´. *Digital three-dimensional image fusion processes for planning and evaluating orthodontics and orthognathic surgery. A systematic review.* J Oral Maxillofac. Surg. 2011; 40: 341–352.

[72] Kau CH, Zhurov A, Richmond S, Bibb R, Sugar A, Knox J, Hartles F. *The 3-dimensional construction of the average 11-year-old child face: a clinical evaluation and application.* J Oral Maxillofac Surg 2006; 64:1086-92.

[73] Nguyen CX, Nissanov J, Ozturk C, Nuveen MJ, Tuncay OC. *Three-dimensional imaging of the craniofacial complex.* Clin Orthod Res 2000; 3:46-50.

[74] Tuncay OC. *Three-dimesional imaging and motion animation.* Sein Orthod 2001; 7:244-50.

[75] Hammond P, Suttie M. *Large-scale objective phenotyping of 3D facial morphology.* Hum Mutat 2012; 817-25.

[76] Heike CL, Upson K, Stuhaug E, Weinberg SM. *3D digital stereophotogrammetry: a practical guide to facial image acquisition.* Head Face Med 2010; 6:18.

[77] Alridge K, Boyadjiev SA, Capone GT, DeLeon VB, Richtsmeier JT. *Precision and error of three-dimensional phenotypic measures acquired from 3dMD photogrammetric images.* Am J Med Genet 2005; 138A:247-53.

[78] Ghoddousi H, Edler R, Haers P, Wertheim D, Greenhill D. *Comparison of three methods of facial measurement.* Int J Oral Maxillofac Surg 2007; 36:250-8.

[79] Gwilliam JR, Cunningham SJ, Hutton T. *Reproducibility of soft tissue landmarks on three-dimensional facial scan.* Eur J Orthod 2006; 28:408-15.

[80] Ras F, Habets LL, van Ginkel FC, Prahl-Andersen B. *Quantification of facial morphology using stereophotogrammtry – demonstration of a new concept.* J Dent 1996; 24:369-74.

[81] Sforza C, Ferrario VF. *Soft-tissue facial anthropometry in three dimensions: from anatomical landmarks to digital morphology in research, clinics and forensic anthropology.* J Anthropol Sci 2006; 84:97-124.

[82] De Menezes M, Rosati R, Allievi C, Sforza C. *A photographic system for the three-dimensional study of facial morphology.* Angle Orthod 2009; 79:1070-7.

[83] Dirven R, Hiigers FJ, Plooji JM, Maal TJ, Berge SJ, Verkerke GJ, Marres HA. *3D stereophotogrammetry for the assessment of tracheostoma anatomy.* Acta Otolaryngol 2008; 128:1248-54.

[84] Schaaf H, Pons-Kuehnemann J, Malik CY, Streckbein P, Preuss M, Howaldt HP, Wilbrand JF. *Accuracy of three-dimensional photogrammetric images in non-synostotic cranial deformities.* Neuropediatrics 2010; 41:24-9.

[85] Van Loon B, van Heerbeek N, Maal TJ, Borstlap WA, Ingels KJ, Schols JG, Bergé SJ. *Postoperative volume increase of facial soft tissue after percutaneous versus endonasal osteotomy technique in rhinoplasty using 3D stereophotogrammetry.* Rhinology 2011; 49:121-6.

[86] Hodges A, Rossouw PE, Campbell PM, Boley JC, Alexander RA, Buschang PH. *Prediction of lip response to four first premolar extractions in white female adolescents and adults.* Angle Orthod 2009; 79:413-21.

[87] Panossian AJ, Block MS. *Evaluation of the smile: facial and dental considerations.* J Oral Maxillofac Surg 2010; 68:547-54.

[88] Swennen GRJ, Schutyser F, Lemaitre A, Malevez C, De Mey A. *Accuracy and reliability of 3-D CT versus 3-D stereo photogrammetry based facial soft tissue analysis*. Int J Oral Maxillofac Surg 2005; 34:73.

[89] Metzger TE, Kula KS, Eckert GJ, Ghoneima AA. *Orthodontic soft-tissue parameters: a comparison of cone-beam computed tomography and the 3dMD imaging system.* Am J Orthod Dentofacial Orthop 2013; 144:672-81.

[90] Groeve PD, Schutyser F, Cleynen- breugel JV, Suetens P. *Registration of 3D photographs with spiral CT images for soft tissue simulation in maxillofacial surgery*. Medical Image Computing and Computer-Assisted Intervention – MICCAI 2001, pp. 991-6.

[91] Galantucci LM. *New challenges for reverse engineering in facial treatments: how can the new 3-D noninvasive surface measurements support diagnosis and treatment?* In: Bártolo PJ, Jorge MA, da Conceicao Batista F, Amorim Almeida H, Matias JM, Correia Vasco J, Brites Gaspar J, Correia MA, Carpinteiro Andre N, Fernandes Alves N, Parente Novo P, Goncalves Martinho P, Carvalho RA,

editors. Innovative Development in Design and Manufacturing. London: Taylor & Francis Group; 2010: pp. 3-12.

[92] Berkowits S, Cuzzi J. *Biostereometric analysis of surgically corrected abnormal faces.* Am J Orthod 1977; 72:526-38.

[93] Moss JP, McCance AM, Fright WR, Linney AD, James DR. *A three-dimensional soft tissue analysis of fifteen patients with Class II, Division 1 malocclusion after bimaxillary surgery.* Am J Orthod Dentofac Orthop 1994; 105:430-7.

[94] Kobayashi T, Ueda K, Honma K, Sasakura H, Hanada K, Nakajima T. *Three-dimensional analysis of facial morphology before and after orthognathic surgery.* J Craniomaxillofac Surg 1990; 18:68-73.

[95] Motegi N, Tsutsumi S, Okumura H, Yokoe Y, Iizuka T. *Morphologic changes in the perioral soft tissue in patients with mandibular hyperplasia using a laser system for three-dimensional surface measurement.* Int J Oral Maxillofac Surg 1999; 28:15-20.

[96] Cevidanes LH, Motta A, Proffit WR, Ackerman JL, Styner M. *Cranial base superimposition for 3-dimensional evaluation of soft-tissue changes.* Am J Orthod Dentofacial Orthop 2010; 137:S120-9.

[97] Rosati R, Manezes M, Rossetti A, Sforza C, Ferrario VF. *Digital dental cast placement in 3-dimensional, full-face reconstruction: a technical evaluation.* Am J Orthod Dentofacial Orthop 2010; 138:84-8.

[98] Boulanger P, Flores-Mir C, Ramirez JF, Mesa E, Branch JW. *Long term three dimensional tracking of orthodontic patients using registered cone beam CT and photogrammetry.* Eng Med Biol Soc 2009; 3525-8.

[99] BaikHS, Kim SY. *Facial soft-tissue changes in skeletal Class III orthognatic surgery patients analysed with 3-dimensional laser scanning.* Am J Orthod Dentofac Orthop 2010; 138:167-78.

[100] Mutsvangwa TE, Veeraragoo M, Douglas TS. *Precision assessment of stereophotogrammetrically derived facial landmarks in infants.* Ann Anat 2011; 193:100-5.

[101] Boehringer S, van der Ljin F, Liu F, Gunther M, Sinigerova S, Nowak S, Ludwig KU, Herberz S, Klein A, Hofman AG, Uitterlinden WJ, Niessen MMB, Breteler A, van der Lugt R, Wurtz RP, Nothen MM, Horsthemke B, Wieczorek D, Mangold E, Kayser M. *Genetic determination of human facial morphology: links between cleft-lips and normal variation.* Eur J Hum Genet 2011; 1192-7.

[102] Gossett CB, Preston CB, Dunford R, Lampasso J. *Prediction accuracy of computer-assisted surgical visual treatment objectives as compared with conventional visual treatment objectives.* J Oral Maxillofac Surg 2005; 63:609-17.

[103] Khambay B, Ullah R. *Current methods of assessing the accuracy of three-dimensional soft tissue facial predictions: technical and clinical considerations.* Int J Oral Maxillofac Surg 2015; 44:132-8.

[104] Nadajimi N, Tehranchi A, Azami N, Saedi B, Mollemans W. *Comparison of soft-tissue profiles in Le Fort I osteotomy patients with Dolphin and Maxilim softwares.* Am J Orthod Dentofacial Orthop 2013; 144:654-62.

[105] Marchetti C, Bianchi A, Muyldermans L, Di Martino M, Lancellotti L, Sarti A. *Validation of new soft tissue software in orthognathic surgery planning.* Int J Oral Maxillofac Surg 2011; 40:26-32.

[106] Shafi MI, Ayoub A, Ju X, Khambay B. *The accuracy of three-dimensional prediction planning for the surgical correction of facial deformities using Maxilim.* Int J Oral Maillofac Surg 2013; 42:801-6.

[107] Bianchi A, Muyldermans L, Di Martino M, Lancellotti L, Amadori S, Sarti A, Marchetti C. *Facial soft tissue esthetic predictions: validation in craniomaxillofacial surgery with cone beam computed tomography data.* J Oral Maxillofacial Surg 2010; 68:1471-9.

[108] Claes P, Walters M, Clement J. *Improved facial outcome assessment using a 3D anthropometric mask.* Int J Oral Maxillofac Surg 2012; 41:324-30.

[109] Metzler P, Bruegger LS, Kruse Gujer AL, Matthews F, Zemann W, Graetz KW, Luebbers HP. *Craniofacial landmarks in young children: how reliable are measurements based on 3-dimensional imaging?* J Craniofacial Surg 2012; 23:1790-5.

[110] Khambay B, Ullah R. *Current methods of assessing the accuracy of three-dimensional soft tissue facial predictions: technical and clinical considerations.* Int J Oral Maxillofac Surg 2015; 44:132-8.

[111] Lundström A, Lundström F, Lebret LM, Moorrees CF. *Natural head position and natural head orientation: basic considerations in cephalometric analysis and research.* Eur J Orthod 1995; 17:111-20.

[112] Morrees CF, Kean MR. *Natural head position: A basic consideration in the interpretation of cephalometric radiographs.* Am J Phys Anthropology 1958; 16:213-34.

[113] Cassi D, De Biase C, Tonni I, Gandolfini M, Di Blasio A, Piancino MG. *Natural head position of the head: review of two-dimensional and three-dimensional methods of recording.* Br J Oral and Maxillofac Surg 2016; 54:233-40.

[114] Cooke MS. *Five-year reproducibility of natural head posture: a longitudinal study.* Am J Orthod Dentofacial Orthop 1990; 97:489-94.

[115] Ferrario VF, Sforza C, Germanò D, Dalloca LL, Miani AJ. *Head posture and cephalometric analyses: an integrated photographic/radiographic technique.* Am J Othod Dentofacial Orthop 1994; 106:257-64.

[116] Peng L, Cooke MS. *Fifteen-year reproducibility of natural head posture: a longitudinal study.* Am J Orthod Dentofacial Orthoped 1999; 116:82-5.

[117] Solow B, Tallgren A. *Natural head position in standing subjects.* Acta Odontol Scand 1971; 29:591-607.

[118] Preston CB, Evans WG, Todres JI. *The relationship between ortho head posture and head posture measured during walking.* Am J Orthod Dentofacial Orthop 1997; 111:283-7.

[119] Bister D, Edler RJ, Tom BD, Prevost At. *Natural head posture- considerations of reproducibility.* Eur J Orthod 2002; 24:457-70.

[120] Jiang J, Xu,T, Lin J. *The relationship between estimated and registered natural head position.* Angle Orthod 2007; 77:1019-24.

[121] Sierbaek-Nielsen S, Solow B. *Intre- and interexaminer variability in head posture recorded by dental auxiliaries.* Am J Orthod 1982; 82:50-7.

[122] Hsung TC, Lo J, Li TS, Cheung LK. *Recording of natural head position using stereophotogrammtry: a new technique and reliability study.* J Oral Maxillofac Surg 2014; 72:2256-61.

[123] Weber DW, Fallis DW, Packer MD. *Three-dimensonal reproducibility of natural head position.* Am J Orthod Dentofac Orthop 2013; 143:738-44.

[124] Hoogeveen RC, sanderink GC, Berkhout WE. *Effect of head position on cephalometric avaluation of the soft-tissue facial profile.* Dentomaxillofac Radiol 2013; 42:20120423.

[125] Hsung TC, Lo J, Li TS, Cheung LK. *Recording of natural head position using stereophotogrammtry: a new technique and reliability study.* J Oral Maxillofac Surg 2014; 72:2256-61.

[126] Zhu S, Keeling A, Hsung TC, Yang Y, Khambay B. *The difference between registered natural head position and estimated natural head position in three dimension.* Int J Oral Maxillofac Surg 2017; http://dx.doi.org/10.1016/j.ijom.2017.07.016

[127] Hughes GN, Gateño J, English JD, Teichgraeber JF, Xia JJ. *There is variability in our perception of the standard head orientation.* Int J Oral Maxillofac Surg 2017; doi: 10.1016/j.ijom.2017.04.023.

[128] Maal TJ, Verhamme LM, van Loon B, Plooij JM, Rangel FA, Kho A, Bronkhorst EM, Bergé SJ. *Variation of the face in rest using 3D stereophotogrammetry.* Int J Oral Maxillofac Surg 2011; 40:1252-7.

[129] http://www.polishape3d.it

[130] Galantucci L. M., Lavecchia F., Percoco G., Raspatelli S. *New method to calibrate and validate a high-resolution 3D scanner, based on photogrammetry*. Precision Engineering 2014; 38:279-91.

[131] Weinberg SM, Scott NM, Neiswanger K, Brandon CA, Marazita ML. *Digital Three-Dimensional Photogrammetry: Evaluation of Anthropometric Precision and Accuracy Using a Genex 3D Camera System.* Cleft Palate Craniofac J 2004; 41:507-18.

[132] Luebbers HT, Messmer P, Obwegeser JA, Zwahlen RA, Kikinis R, Graetz KW, Matthews F. *Comparison of different registration methods for surgical navigation in cranio-maxillofacial surgery.* J Craniomaxillofac Surg 2008;36:109-16.

[133] Marmulla R, Muhling J, Eggers G, Hassfeld S. *Markerless patient registration. A new technique for image-guided surgery of the lateral base of the skull.* HNO 2005; 53:148-54.

[134] Prof. Joe Abramson, 2016, http://www.brixtonhealth.com/pepi4windows.html

[135] Baysal A, Sahan AO, Ozturk MA, Uysal T. *Reproducibility and reliability of three-diemnsional soft tissue landmark identification using three-dimensional sterophotogrammetry.* Angle Orthod 2016; 86:1004-9.

[136] Alridge K, Boyadjiev SA, Capone GT, DeLeon VB, Richtsmeier JT. *Precision and error of three-dimensionsl phenotypic measures acquired from 3dMD photogrammetric images.* Am J Med Genet 2005;138A:247-53.

[137] Lubbers H-T, Medinger L, Kruse A, Gratz KW, Matthews F. *Precision and accuracy of the 3dMD photogrammetric system in craniomaxillofacial application.* J Craniofac Surg 2010; 21:763-67.

[138] Ayoub A, Garrahy A, Hood C, White J, Bock M, Sieber JP, Spencer R, Ray A. *Validation of a vision-based, three-dimensional facial imaging system.* Cleft Palate Craniofac J 2003; 40:523-9.

[139] Jhonston DJ, Millett DT, Ayoub AF, Bock M. *Are facial expression reproducible?* Cleft Palate Craniofac J 2003; 403:291-6.

[140] Zhu S, Keeling A, Hsung TC, Yang Y, Khambay B. *The difference between registered natural head position and estimated natural head position in three dimension.* Int J Oral Maxillofac Surg 2017; http://dx.doi.org/10.1016/j.ijom.2017.07.016

[141] Hughes GN, Gateño J, English JD, Teichgraeber JF, Xia JJ. *There is variability in our perception of the standard head orientation.* Int J Oral Maxillofac Surg 2017; doi: 10.1016/j.ijom.2017.04.023.

[142] Maal TJ, Verhamme LM, van Loon B, Plooij JM, Rangel FA, Kho A, Bronkhorst EM, Bergé SJ. *Variation of the face in rest using 3D stereophotogrammetry.* Int J Oral Maxillofac Surg 2011; 40:1252-7.